Temporal gene expression of *Chlamydia trachomatis* in keratinocytes at 37º versus 33ºC

Submitted by: Gugulethu F. Mzobe

Supervisor: Dr B.C Joubert

Co-supervisor: Professor A.W Sturm

Submitted in fulfillment of the requirements for the degree of Doctor of Philosophy in the Discipline of Medical Microbiology and Infection Control, School of Laboratory Medicine and Medical Sciences, University of KwaZulu-Natal

PREFACE

The experimental work described in this thesis was carried out in the Infection Prevention and Control Laboratory, Doris Duke Medical Research Institute Building, Nelson R Mandela School of Medicine, University of KwaZulu -Natal, South Africa under the supervision of Dr Bronwyn Joubert and co-supervision of Professor Willem Sturm.

This study represents the original work by the author and has not otherwise submitted in any form to any other university. Where use of the work of others has been made, it is duly acknowledged in the text.

06 September 2017

Gugulethu Mzobe (candidate) Date

Dr B.C Joubert (supervisor) Date

Professor A.W Sturm (co-supervisor) Date

PLAGIARISM DECLARATION

I, **Gugulethu Mzobe** declare that

I. The research reported in this thesis, except where otherwise indicated, is my original work.

II. This thesis has not been submitted for any degree or examination at any other university.

III. This thesis does not contain other person's data, pictures, graphs or other information, unless specifically acknowledged as being sourced from other persons.

IV. This thesis does not contain other person's writing, unless specifically acknowledged as being sourced from other researchers. Where other written sources have been quoted, then:

a) Their words have been rewritten but the general information attributed to them has been referenced;

b) Where their exact words have been used, their writing has been placed inside quotation marks, and referenced.

c) Where I have reproduced a publication of which I am an author, co-author or editor, I have indicated in detail which part of the publication was actually written by myself alone and have fully referenced such publications.

V. This thesis does not contain text, graphics or tables copied and pasted from the Internet, unless specifically acknowledged, and the source being detailed in the thesis and in the References sections.

Signed:  Date: 06 September 2017

ETHICAL APPROVAL

This study was approved by the Biomedical Research Ethics Committee of the University of KwaZulu-Natal (REF: BE220/13).

ACKNOWLEDGEMENTS

- I would like to express my sincere gratitude to my supervisors Dr. B.C Jourbert and Prof A.W Sturm for their guidance, continuous support of my PhD study and for teaching me so much in the field of Medical Microbiology
- Microscopy and Microanalysis Unit (MMU) staff at UKZN Westville campus for their assistance with the use of the transmission electron microscopy
- Department of Infection Prevention and Control (UKZN)
- The National Research Foundation (NRF) for funding
- University of KwaZulu-Natal College of Health Sciences (CHS) for funding

LIST OF FIGURES AND TABLES

redifferentiation at 37°C and 33°C over the course of the developmental cycle. Uninfected (A), 2h (C), 12h (E), 24h (G), 36h (I) and 48h (K) post infection at 37°C. Uninfected (B), 2h (D), 12h (F), 24h (H), 36h (J), 48h (L), 60h (M) and 72h (N). Cultures in C-E and D-F were infected at an MOI of 100 to increase the likelihood of visualizing organisms in thin sections. Cultures in G-K and H-N were infected at an MOI of 10. Cultures in G-N were infected at an MOI of 10. Bar, 500 nm.

LIST OF ABBREVIATIONS

ABI	Applied Biosytems
ATCC	American Type Culture Collection
ATP	Adenosine triphosphate
CCM	Cell culture medium
cDNA	Complementary deoxyribonucleic acid
CGM	Chlamydia growth medium
CTPK	*Chlamydia trachomatis* pyruvate kinase
DEPC	Diethylpyrocarbonate
DNA	Deoxyribonucleic acid
dNTP	Deoxynucleoside triphospate
EB	Elementary body
EDTA	Ethylenediaminetetraacetic acid
EMEM	Eagle's minimum essential medium
FBS	Fetal bovine serum
FITC	Flourescein isothiocynate
F26BP	Fructose-2, 6-biphosphate
GTC	Guanadine thiocyanate
HctA	Histone-like proteinA
Inc	Inclusion membrane protein
IFU	Inclusin Forming Unit
LGV	Lymphogranuloma venereum
MOI	Multiplicity of infection
MOMP	Major outer membrane protein
OmcB	Outer membrane complex protein B
PBS	Phosphate buffer saline

Pyk	Pyruvate kinase
RB	Reticulate body
RNA	Ribonucleic acid
RPMI	Roswell Park Memorial Institute
RT-PCR	Real-time polymerase chain reaction
SPG	Sucrose-phosphate-glutamate
Tal	Transaldolase
TEM	Transmission electron microscopy
μm	micrometer

ABSTRACT

Introduction/Aim

Keratinocytes are the first port of entry for *Chlamydia trachomatis* of the lymphogranuloma venereum (LGV) biovar which causes LGV. However LGV pathogenesis and gene expression studies are usually performed in cells which are not the native host cells. In this study we investigated chlamydial gene expression in a keratinocyte cell line at both core (37°C) and skin (33°C) temperature in an attempt to understand what happens *in vivo.*

Methods

C. trachomatis infected HaCaT cells were incubated at either 33ºC or 37ºC. The level of expression of six genes which are known to be expressed at different times during the chlamydial lifecycle was quantified relative to a house keeping gene (16s rRNA). Transmission electron microscopy (TEM) was performed to confirm the stage of the developmental cycle that the organism was at inside the keratinocytes. The results of the gene expression assays were compared with TEM done under the same conditions.

Results

As expected, the early cycle genes *groEL* and *incB* were expressed throughout the life cycle at both temperatures for all the chlamydial strains tested. At 37ºC, L2 434 showed an over 30-fold increase in *incB* expression level at 2 hours post infection, compared to L2 US151 in which a constantly lower level of expression was observed.

Pyk-F expression was most abundant at 2 hours post infection at 37ºC in all tested chlamydial strains. *Tal* on the other hand was expressed the highest at 12 hours post infection for strain E, which correlates with rapid growth and division of RBs. This was consistent with the electron microscopic observations. At 33ºC, both *pyk-F* and *tal* were most abundant from 24 hours post infection. This was also consistent with the TEM observations in which the metabolically active RB form was only observed from 24 hours post infection at 33ºC. At 37ºC an increase in *hctA* expression was observed at 2

hours post infection and decreased by 1- fold at 12 hours post infection for L2 434 and serovar E. At 33^{o}C; *hctA* expression was abundant from 24 hours post infection for L2 434 and US151, although *hctA* was still expressed in low levels at 2 and 12 hours post infection. Strain E had two expression peaks of *hctA*, at 24 and 72 hours post infection. Like *hctA*, at 37^{o}C strain L2 434 showed high *omcB* expression level at 2 hours post infection. At 12 hours post infection the expression level was suppressed, but upregulated again at 24 hours post infection. At 33^{o}C, Both L2 reference strains and strain E only expressed *omcB* from 24 hours post infection and increased at 36 hours post infection. This was consistent with the TEM, which showed numerous EBs at 36 hours post infection.

Discussion/Conclusion

This study confirms that mid and late-cycle chlamydial gene expression levels are different to the published research conducted in HeLa cells at 37^{o}C.and that temperature has an effect on the level of chlamydial gene expression when grown in keratinocytes. At 2 hours post infection chlamydia still retains its EB structural conformation in keratinocytes at 37^{o}C. The L2 reference strain 434 is different than the clinical L2 US151as indicated by the difference in the gene expression pattern.

CHAPTER 1: INTRODUCTION

Chlamydia trachomatis is an obligate intracellular gram-negative bacterium, which is associated with various sexually transmitted diseases.

The species *Chlamydia trachomatis* is traditionally subdivided into two biovars: the lymphogranuloma venereum (LGV) and oculogenital (OG) biovar. This is based on the differences in disease manifestation (Ward 1983). The differences in clinical disease of the OG biovar as well as differences in the variable region of the chlamydia genome, known as the plasticity zone, indicate that *C. trachomatis* should be divided into three biovars: trachoma/oculo (O), genital (G) and LGV biovar (Carlson, Porcella et al. 2005). Strains of the LGV biovar target the keratinocytes in the primary stage of infection whereas G biovar strains target cervical and urethral epithelial cells (Joubert 2010).

Chlamydia are characterized by a unique two-phase developmental cycle. In the extracellular phase, the organism manifests as the elementary body (EB). This EB is infectious and metabolically inactive. Once the EB is endocytosed it differentiates into the metabolically active reticulate body (RB) which replicates within inclusions by binary fission (Hanada, Ikeda-Dantsuji et al. 2003). The chlamydia revert back into the metabolically inactive EB that is released from the host cell to infect additional cells in the same or in the next host (Beagley and Timms 2000, Sherrid and Hybiske 2017). Chlamydia were previously thought to be viruses because of their obligate intracellular life cycle. Until recently, chlamydia were described as true energy parasites in that they require both energy (ATP) and nutrients from the host cell and that they are not capable of *de novo* nucleotide synthesis and must rely on host nucleotides for replication (Black 1997).

Keratinocytes are the first port of entry for *Chlamydia trachomatis* of the LGV biovar, which causes lymphogranuloma venereum (LGV). LGV is an invasive, sexually transmitted disease of humans, which begins as an ulcer in the genital region. The chlamydia of the LGV biovar infect viable keratinocytes in the stratum spinosum and basale of the epidermis. The ulcers that appear vary in size and tend to heal spontaneously. From these skin lesions, the bacteria migrate to the inguinal lymph nodes causing lymphadenopathy. LGV pathogenesis and gene expression studies are usually performed in cells other than keratinocytes that are not the native host cells. Furthermore, the initial site of infection, the skin, and the secondary site of infection, the inguinal lymph nodes have different temperatures. The temperature of human skin (port of entry) is 33°C, while the temperature of the inguinal lymph nodes is 37°C. Most previous studies have only focused on the latter temperature. Joubert and Sturm (2011) have demonstrated that *C. trachomatis* does infect keratinocytes *in vitro* both at 37°C and 33°C, although they replicate faster at 37°C than at 33°C. This study aims to determine the relative level of expression of two early, two mid-cycle and two late-cycle chlamydial genes (Shaw, Dooley et al. 2000) when grown in keratinocytes, to compare the differences in the expression of these genes at 37^{o} versus 33°C and to compare the gene expression results to the level of morphological differentiation by means of electron microscopy.

To date there have been no gene expression studies of chlamydia in keratinocytes, which is the first target of infection for organisms of the LGV biovar, and no studies have compared gene expression at core (37°C) versus surface temperature (33°C) of the human host.

CHAPTER 2: LITERATURE REVIEW

2.1 Classification of *Chlamydia trachomatis*

Chlamydia constitute one of the most successful groups of obligate intracellular bacteria. Over the past 10 years, the taxonomy and nomenclature of the chlamydia have changed. Originally, *Chlamydia trachomatis* and *Chlamydia psittaci* were the only two species that were under the order *Chlamydiales*, family *Chlamydiaceae* and genus *Chlamydia*. The genus Chlamydia is characterized by its unique developmental cycle (Debattista, Timms et al. 2003) and the two species were distinguished based on their characteristics such as sensitivity to sulfodiazine, host range and the buildup of glycogen within the chlamydial inclusions. Two other species were later recognised, *Chlamydia pneumoniae* in 1989 and *Chlamydia perocum* in 1992. Both these species were subgroupings within *C. psittaci (Black 1997).*

For many years *C. trachomatis* was subdivided into two biovars: the oculogenital or OG biovar and the lymphogranuloma venereum orLGV biovar. Currently genotyping, based on the gene encoding MOMP, is more commonly with ompA genotypes A–C associated with trachoma, D–K with urogenital infections, and L1–L3 with LGV. Recent publications have confirmed previous findings that ompA is not a reliable marker of phylogeny due to extensive recombination within the genomes of *C. trachomatis* strains (Seth-Smith, Harris et al. 2013)

Over the past 5 years, the use of molecular methods has led to the discovery of more phylogenic groupings within the *Chlamydiaceae* family. Based on sequence analysis of the 16SrRNA and 23SrRNA genes it has been proposed to divide the C*hlamydiaceae*

family into two genera: *Chlamydia* and *Chlamydophila*. Together, these two genera harbour nine species (Table 2.1) (Everett, Bush et al. 1999, Beagley and Timms 2000).

Table 2.1: Chlamydiaeceae genera and species

Genus	**Species**	**Host infected**	**Diseases caused**
Chlamydia	*C. trachomatis*	Humans	sexually transmitted diseases, trachoma, neonatal conjunctivitis
	C. muridarum	mice, hamsters	respiratory infections, pneumonia, ileitis
	C. suis	Swine	conjunctivitis, enteritis, pneumonia
	C. abortus	cattle, sheep, goats	abortion
	C. psittaci	humans, birds	pscittacosis, systemic disease
	C. caviae	guinaea pigs	genital tract infections, conjunctivitis
	C. felis	Cats	conjunctivitis, rhinitis
	C. percorum	cattle, sheep, goats, koalas, swine	reproductive disease, conjunctivitis, abortion, pneumonia, encephalomyelitis, enteritis
	C. pneumoniae	humans, horses, koalas	pneumonia, other respiratory tract infections

2.2 Disease manifestations associated with chlamydia

Among the strains of *C. trachomatis*, there are 15 serovars based on the differences in the epitopes found on the major outer membrane protein (MOMP): 3 lymphogranuloma

venereum (L1 to L3) and 13 oculogenital serovars (A, B, Ba, C, D, Da, E, F, G, H, I, J and K) (Ward 1983).

Of the sexually transmitted chlamydia, the genital biovar consisting of serovars D-K is most common. It causes urethritis, epididymitis and prostatitis in male and cervicitis, urethritis and pelvic inflammatory disease in female. The genital biovar is also found as a cause of conjunctivitis in neonates born from chlamydia infected mothers (SHERMAN, DALING et al. 1990, Fredlund, Falk et al. 2004)

The LGV strains are different from other strains of *C. trachomatis* in that they are more invasive, resulting in initial infection of the epithelial layers followed by spread in the lymphatic tissue (Söderlund and Kihlström 1982) (Bébéar and De Barbeyrac 2009). The classic presentation of LGV consist of three stages. The primary stage is a painless genital ulcer that evolves into the secondary stage, which is inguinal lymphadenopathy. This is followed by genito-anorectal syndrome, which is the tertiary stage (Schachter and Osoba 1983). Not all stages are seen in each patient.

2.3 Pathogenesis of chlamydial infection

C. trachomatis exercises its pathogenicity during its interaction with the host cell and when it is released from the infected cell to infect further uninfected host cells. Like most intracellular organisms, chlamydia escape defence mechanisms of the host by its intracellular lifestyle in which the cell provides a protective environment (Beatty, Morrison et al. 1994, Belland, Zhong et al. 2003, Frohlich, Hua et al. 2014).

The infectious chlamydial form, the elementary body (EB), adheres to the host cell membrane and initiates entry. The membrane of the EB contains proteoglycan, a ligand through which the EB attaches to microvilli of the host cell and is subsequently

embedded in clathrin-coated vesicles. Within the host cell, the EB remains within the non-acidic intracellular vacuole, avoiding fusion of the phagocytic vesicle with the host cell lysosome, thus allowing it to escape the endocytic pathway and establishing fusogenicity sphingomyelin-containing exocytic vesicles, called inclusion bodies (Hackstadt, Scidmore et al. 1995, Shaw, Dooley et al. 2000, Wyrick 2010). These chlamydia containing inclusion bodies are then redistributed from the cell periphery to the area around the nucleus.

Under stressful conditions in vitro, *C. trachomatis* can enter into an alternative viable but non-dividing growth form, known as the persistent growth form (Beatty, Morrison et al. 1994, Frohlich, Hua et al. 2014). Persistent growth of chlamydia may correlate to a reduction in metabolic activity, which restricts growth and division and delays differentiation to mature EBs. Limited metabolic capacity may also influence the biochemical and antigenic attributes of the persisting organisms, potentially rendering them undetectable by normal diagnostic tests (Beatty, Morrison et al. 1994). This persistent growth state has been suggested to be linked to chronic infection and unfavourable outcomes, including stimulation of tissue damaging host responses (Darville and Hiltke 2010). Persistent forms are also less responsive to antimicrobial therapy *in vitro* and *in vivo* (Phillips-Campbell, Kintner et al. 2014).

2.4 Morphology

Chlamydia display a life cycle that involves the consecutive alternation of two distinct morphological forms, the elementary body (EB) and the reticulate body (RB).

2.4.1 Architecture of cell envelope

One of the important developmental events shared by chlamydia species is the ability

of the organisms to adapt their envelopes for the purpose of interacting with the host cell. Like other Gram-negative bacteria, the *C. trachomatis* envelope consists of an outer membrane (OM), an inner membrane (IM), and a periplasm (Frohlich, Hua et al. 2014). Recent studies by (Pilhofer, Aistleitner et al. 2013, Liechti, Kuru et al. 2014) have shown that chlamydia have a functional peptidoglycan (PG). The existence of PG has long been debated. Whereas genetic analysis and susceptibility to antibiotics indicate the presence of PG, yet all attempts to detect PG have proven unsuccessful, resulting in the 'chlamydial anomaly' (Moulder, Novosel et al. 1963, Tamura and Manire 1968, Stephens, Kalman et al. 1998). Liecthi, et al (2014) have recently demonstrated the presence of PG in *C. trachomatis* by a new metabolic cell wall labelling method and observed that chlamydial PG is present in a ring-like structure at the apparent cell division plane and does not appear as a sacculus form.

The chlamydial envelope possesses a cross-linked outer membrane protein (MOMP), which is a unique feature that distinguishes chlamydia from other Gram-negative bacteria. The most exposed surface molecule of both EBs and RBs is the MOMP and this functions as an adhesin and as a porin (Caldwell, Kromhout et al. 1981, Wang, Berg et al. 2006). MOMP is also capable of adapting to different chlamydial stages by altering its conformation (Feher, Randall et al. 2013). MOMP contains cysteine rich omcB and omcA. These cross-linked cysteine rich proteins contribute in osmotic stability and cell rigidity of the EBs (Frohlich, Hua et al. 2014).

2.4.2 Elementary body

The elementary body (EB) is the extracellular, infectious and metabolically inactive form of the chlamydia which is responsible for attaching to the target host cell (Ward

1983, Beatty, Morrison et al. 1994). EBs are 0.2 – 0.3 μm in diameter and are rigid, allowing them to be osmotically stable, to endure environmental stress and to survive after lysis of the host cell (Ward 1983). EBs have highly condensed DNA in an electron-dense nucleoid which is detectable by transmission electron microscopy (Siegl, Horn et al. 2012). EBs have highly cross-linked disulfide bonds on the MOMP formed by two cysteine rich proteins. These are a 60 kDa envelope protein and 12 kDa outer membrane lipoprotein, which enhance structural stability and enables the EB to attach to and enter host cells (Sardinia, Segal et al. 1988). The role of EBs is to allow spread of chlamydial infection from one cell to another (Beatty, Morrison et al. 1994).

2.4.3 Reticulate body

The reticulate body (RB) is the intracellular, non- infectious and replicative form of chlamydia which cannot survive outside the host cell (Beatty, Morrison et al. 1994). RBs are larger in diameter than EBs (~1μm). Their cell wall is fragile and osmotically sensitive, probably because of the absence of cross-linked disulfide bonds on the MOMP. The MOMP forms pores that provide a passageway for nucleotides, metabolites and ATP from the host cell to the chlamydial cell. Protein synthesis in RBs depends on the ATP-ADP exchange mechanism not possessed by EBs (Moulder 1991). They also have dispersed DNA; allowing activation of DNA signals, chlamydial protein synthesis and RB replication. RBs contain endosome intercepts for expansion of the membrane bound vesicle called an "inclusion" to accommodate the increasing number of replicating RBs (Wyrick 2010).

2.5 The life cycle of chlamydia

Chlamydia are characterized by a unique two-phase developmental cycle comprising two cell types; EBs and RBs. EBs are incapable of dividing. They are released from infected cells to infect adjacent host cells, where they transform into RBs. RBs are incapable of infecting new host cells, they replicate and eventually rearrange into a new population of EBs. The entire cycle takes place within a vacuole termed an inclusion (Shaw, Dooley et al. 2000).

Infection is induced following the attachment of an EB to the host cell. The internalization of LGV strains into a target cell is not dependent on the cytoskeleton, whereas internalization of OG strains is enabled by microvilli (Schramm and Wyrick 1995, Wyrick 2010). EB remain in an inclusion, which does not fuse with the host cell lysosome (Hammerschlag 2002). Within the first 2 to 6 h post infection, differentiation of EB into RB begins. During this transition the organism loses its infectivity, increases in size, its chromosome is decondensed and there is an increase in metabolic activity (Moulder 1991, Belland, Zhong et al. 2003). RBs replicate within inclusions by binary fission, forming a microcolony. As this microcolony grows, the inclusion membrane expands to accommodate the differentiating RBs. After 18 to 24 h post infection the numbers of RBs have increased and they start to revert back to the EB form, which accumulate in the lumen of the inclusion as the remaining RBs continue multiplying (Shaw, Dooley et al. 2000, Nicholson, Olinger et al. 2003). Depletion of nutrients and ATP during replication of RBs serve as a signal for RBs to mature and reorganize back to infectious EB (Wyrick 2010). Approximately 48 h post infection the cell lyses and releases mature EBs to infect more host cells (Belland, Zhong et al. 2003). With the OG strains, release is through exocytosis while LGV strains are released through cell

cytolysis (Todd and Caldwell 1985). Extrusion of the entire inclusion may occur, resulting in a silent, chronic infection (Hammerschlag 2002).

2.5.1 Attachment and ingestion

The surfaces of EBs are hydrophobic and negatively charged at a neutral pH. Host cells are also negatively charged at pH 7. The negatives charges on the surfaces of both chlamydia and the host cell mainly represent free carboxyl groups. With both interacting surfaces carrying a net negative charge, the question arises as to how chlamydia ever attach to the host cells. It has been suggested that the neutralization of the chlamydial ligands by electrostatic interaction with the host cell ligands results in the binding of chlamydia to the host cell by Van der Waals forces (Moulder 1991). Entry of the EB is promoted by actin cytoskeleton in the cell wall (Carabeo, Grieshaber et al. 2002). As soon as an inclusion is formed, entry of additional EBs into that host cell is blocked (Moulder 1991).

2.5.2 Metabolic capacity

Previously it was believed that chlamydia lack the enzymes required for ATP synthesis, therefore making the intracellular developmental cycle dependent on ATP obtained from the host cell and possibly on a number of other host-acquired high-energy metabolites.

However, recent findings suggest that chlamydia may not live as energy parasites throughout the developmental cycle and that elementary bodies are not metabolically inert but exhibit metabolic activity under appropriate axenic conditions (Omsland, Sager et al. 2012, Omsland, Sixt et al. 2014).

Chlamydia contain genes that code for the enzymes for conversion of glucose-6-phosphate to pyruvate via glycolysis. This allows them to generate ATP via substrate level phosphorylation by the enzymes phosphoglycerate kinase and pyruvate kinase. To determine whether chlamydia contains functional enzymes involved in a glycolysis or pentose phosphate pathway (PPP), four enzymes involved in glycolysis and PPP were cloned, sequenced and expressed as recombinant proteins in *E. coli*. The deduced amino acid sequences showed high homology to other enzymes of glycolysis and PPP (Iliffe- Lee and McClarty 1999).

The TCA cycle is known to be incomplete in the *Chlamydiaceae* family due to the absence of the enzymes citrate synthase (*GltA*), aconitase (*Acn*), and isocitrate dehydrogenase (*Icd*) (Carlson, Porcella et al. 2005). Therefore, a constant metabolite exchange with the host cell is required to initiate the TCA cycle (Stephens, Kalman et al. 1998).

2.6 Gene expression

Previous gene expression studies have only been performed in either HeLa or Hep-2 cell lines at 37^{o}C and have shown that a number of chlamydial genes are temporally expressed during the developmental cycle. The mechanism of regulation is largely unknown. Analysis performed by Shaw *et al*., (2000) and Belland *et al*., 2003 suggested that *C. trachomatis* transcription occurs in three temporal phases: early (2 h post infection), mid- cycle (6- 18 h post infection), and late (24- 48 h post infection). Gene products are only transcribed temporarily when they are required in the developmental cycle (Niehus, Cheng et al. 2008). Transcription begins instantly after internalization.

De novo transcription and translation are required to facilitate and coordinate molecular events occurring during the developmental cycle (Abdelrahman and Belland 2005).

2.6.1 Early gene expression

As the chlamydial developmental cycle begins, the formation and modification of the unique intracellular niche, called an inclusion, also occurs. The inclusions are non-fusogenic with host lysosomes. The inclusion membrane is significantly modified by a set of chlamydial proteins collectively known as Incs which are assumed to be significant in chlamydial pathogenesis (Fields, Fischer et al. 2002). It is hypothesized that Inc proteins are involved in the trafficking and fusion of chlamydial inclusions (Shaw, Dooley et al. 2000). When the inclusions are trafficked along microtubules they associate with the host-derived lipids to sustain integrity as they increase in size during RB replication

The Inc proteins belong to a class of proteins expressed early in the chlamydial developmental cycle. Among the early events of chlamydial infection is extensive modification of the inclusion membrane by the insertion of a number of type III secreted effector proteins (Mital, Miller et al. 2013). Studies have shown the presence of several Incs located in the inclusion membrane. These Inc proteins lack primary sequence homology; however, they are all characterized by the absence of an N-terminal and the presence of bi-lobed hydrophobic domains comprising 40 to 60 amino acid residues (Pannekoek, van der Ende et al. 2001, Fields, Fischer et al. 2002).

The chlamydial heat shock protein GroEL is another example of protein expressed early in the chlamydial developmental cycle (Karunakaran, Noguchi et al. 2003) and

represent macromolecular biosynthetic and protein processing pathways because they produce the ∝ subunit of DNA polymerase (Shaw, Dooley et al. 2000). GroEL expression increases during a variety of conditions such as heat shock, nutrient deprivation, infection, and inflammatory reaction and functions to stabilize cellular proteins (Young and Elliott 1989). GroEL proteins are highly conserved in sequence among bacteria and are recognized in the host by Toll-like receptors as part of an innate defense system (Karunakaran, Noguchi et al. 2003).

2.6.2 Mid-cycle gene expression

During the mid-cycle the transition of infectious EB into non-infectious, metabolically active RB occurs. RB replicate within an inclusion by binary fission until late in the infection (Shaw, Dooley et al. 2000).

Genes expressed in the mid-cycle are associated with energy metabolism. An example of mid-cycle genes is pyruvate kinase (*pyk*), an enzyme of glycolysis which catalyzes the irreversible conversion of phosphoenolpyruvate to pyruvate with the release of ATP (Mathews, George et al. 2001). This reaction is a main regulatory point in the glycolysis pathway which controls the flux of the glycolytic intermediates and regulates the level of ATP in the cell (Fothergill-Gilmore and Michels 1993). Pyk enzymes can be classified as type I pyk and type II pyk. Type I pyk is dominant during glycolysis, where it is activated by fructose -1, 6- bisphosphate (F16BP). Type II pyk is dominant during gluconeogenesis, where it is activated by AMP, ribose -5-phosphate (R5P) and glucose -6-phosphate (G6P) (Iliffe- Lee and McClarty 2002).

Chlamydia trachomatis pyruvate kinase (CTPK) is an allosteric enzyme that is 53.5 kDa with a pH of 7.3 and requires monovalent (K^+) and divalent (Mg^{2+}) for its activity. CTPK has been discovered to be the only known bacterial Pyk that is allosterically

activated by fructose -2, 6- bisphosphate (F26BP) (Fothergill-Gillmore, Rigden et al. 2000). Chlamydia do not have enzymes to metabolize F26BP. However, according to the information from the chlamydial genomic sequence, chlamydia do contain a small number of genes for the biosynthesis of metabolites and the genes for transporters with extensive substrate specificity. This suggests that chlamydia have transport systems for obtaining metabolites from the host. Therefore, chlamydia may acquire F26BP from the host. Sugar monophosphates such as G6P, F6P, R5P can also activate CTPK, thus suggesting that CTPK has properties for both type I and type II Pyk (Iliffe- Lee and McClarty 2002).

Gene encoding transaldolase (*tal*) of the pentose phosphate pathway (PPP) is also detected in the mid-cycle (Shaw, Dooley et al. 2000). This enzyme is important for the balance of metabolites in the PPP by increasing the catabolism of sugars. Transaldolase is involved in step 2 of the sub pathway that synthesizes D-glyceraldehyde 3-phosphate and beta-D-fructose 6-phosphate from D-ribose 5-phosphate. This sub pathway is part of PPP, which is itself part of carbohydrate degradation.

2.6.3 Late gene expression

Late in the chlamydial developmental cycle the non-infectious RB reorganize back into infectious EB. During this process genes encoding structural and regulatory proteins are expressed (Shaw, Dooley et al. 2000).

hctA is an example of the genes expressed late in the chlamydial developmental cycle and it is defined as a lysine rich protein with a primary sequence similar to the eukaryotic histone Hc1(Niehus, Cheng et al. 2008). This histone-like protein is

produced late in chlamydial developmental cycle during the conversion of RB to infectious EB and it mediates the condensation of the chromosome. As RB replication begins during the first few hours of infection, the condensed chromosome of EB is decondensed. The histone-like protein binds to and blocks the *hctA* gene to repress its transcription and translation. IhtA, a small non-coding RNA, regulates expression of this protein. In the early stages of the developmental cycle *IhtA* gene is transcribed and its product, the IhtA regulatory RNA, represses the translation of this IhtA protein, ensuring that it remains low and constant until RB start reorganizing to EB. Transcription of *IhtA* decreases late in the developmental cycle, allowing synthesis of *hctA* (Tattersall, Rao et al. 2012).

The outer membrane complex protein B (omcB) is the most abundant and conserved outer membrane protein in chlamydia (Hou, Lei et al. 2013). OmcB functions as an adhesin during attachment of EB to the host cell and also contributes to osmotic stability and cell rigidity involved in the final stage of the life cycle (Shaw, Dooley et al. 2000). Therefore, *omcB* is expressed late in the chlamydia developmental cycle.

CHAPTER 3: MATERIALS AND METHODS

3.1 Cell culture

3.1.1 Cell line

The HaCaT cell line was used for both propagation of chlamydia and the experimental work. It is a spontaneously immortalized human keratinocyte cell line (Boukamp *et al*. 1988) donated in 1995 by Professor N. E. Fusenig of the Cancer Research Centre, Heidelburg, Germany.

HaCaT cells were cultured in Roswell Park Memorial Institute 1640 (RPMI 1640) medium (Lonza) with HEPES (10 mM), L-glutamine (2 mM) and 10 % foetal bovine serum (FBS) (Biowest). Unless stated otherwise, for all experiments FBS was heat inactivated for 30 minutes at 56^{o}C

3.1.2. Retrieval of frozen cells and maintenance

The cells were stored in cryovials at -80°C until required. When required the cell suspensions were thawed in a 37°C water bath under gentle agitation of the vial. After the cells were thawed, the cryovials were swabbed with 70% alcohol and transferred to a class II biological safety cabinet. The cell suspension was transferred into a 75 cm^2 cell culture flask containing RPMI 1640 supplemented with 10% FBS. The flasks were then incubated at 37°C. The colour of the media was checked and the cells were examined daily using an Olympus IX70-S8F2 inverted phase contrast microscope, in order to monitor the morphology, the density of cell growth and possible signs of contamination. Every 2-3 days the spent media was discarded and the cells were washed

once using phosphate buffered saline, pH 7.2 (PBS) (Oxoid) to wash off unattached cells. Fresh media were added and the monolayers reincubated if necessary.

3.1.3 Trypsinisation and passage

When the monolayers in the tissue culture flasks were approximately 90% confluent, the spent cell culture media (CCM) was siphoned off and the cells were washed three times with PBS to ensure that the FBS from the spent media and all unattached cells were removed. Two millilitres of 0.05 % ethylene-diamine-tetra-acetic acid (EDTA) (Sigma, Steinheim, Germany) were added to the culture flask to completely cover the monolayer. Cells were then incubated at 37°C for 5-10 minutes. EDTA is a calcium chelator which saturates the remaining divalent cations (Mayer, Woods et al. 1993). Progress was checked by examination with the inverted phase contrast microscope. After incubation the cells appeared slightly rounded with small spaces between the cells. The EDTA solution was then removed and discarded. One millilitre of 0.05 % trypsin - 0.02 % EDTA solution in distilled water (Whitehead Scientific - BioWhittaker™) was added to the monolayer to detach the cells. Excess trypsin solution was discarded and the flask returned to the 37°C incubator to activate the trypsin. Once the cells had become visibly rounded in appearance, the side of the flask was gently tapped against the hand to assist detachment of the cells. If trypsin is allowed to stay in contact with the cells for too long, the ability of the cells to attach to a new surface is reduced (Joubert 2010). One millilitre of FBS was then added to the flask to deactivate the trypsin. This cell suspension was seeded in new culture vessels for propagation, seeded in multi-well plates for experimental work or cryopreserved for later use.

3.1.4 Cryopreservation of cells

After trypsinization an equal volume of cryopreservation fluid was slowly added to the cell suspension. Cryopreservation fluid for HaCaT cells contains 60% RPMI 1640, 20% glycerol (BDH Laboratory Suppliers) and 20% FBS. The mixture of cell suspension and cryopreservation fluid was then aliquoted into cryovials, labelled with the name of the cell type, passage number and date. Cells were allowed to freeze slowly overnight in an enclosed polystyrene rack at -80°C. The following morning the vials were transferred to a storage box and kept at -80°C.

3.1.5 Determination of cell numbers

The Neubauer haemocytometer was used to perform the Trypan Blue Exclusion assay. This was used to determine the total number of cells and viable cell numbers. Twenty microliters of cell suspension prepared as described in section 3.1.3 was added to 20 µl of 0.4 % trypan blue solution (Sigma, Steinheim, Germany). A cover slip was placed over the haemocytometer and a small amount of the trypan blue-cell suspension was transferred to each chamber of the haemocytometer by touching the edge of the cover slip with the pipette tip and allowing the chamber to fill by capillary action. The contents of the haemocytometer was then viewed under a bright field microscope (Nikon P60) at 40x magnification and the cells were enumerated. Viable cells appeared colourless because they can actively pump out the dye. The non-viable cells retained the blue colour because they are unable to pump out the dye (Pauwels et al., 1988). The number of cells per ml and percentage viability was calculated as follows:

Concentration (cells/ml) = average cell count per primary square X dilution factor $X10^4$

Total cell number = concentration x total volume

$$\% \text{ cell viability} = \frac{\text{total viable cells (unstained)}}{\text{total cells}} \times 100$$

3.2 *Chlamydia trachomatis* culture

Three isolates were used for the experiments: the L2 reference strain 434 (ATCC® VR-902B™), one serovar L2 clinical isolate (US151) and one serovar E clinical isolate. US151 was grown by Joubert, 2009 from the ulcer specimen of a male patient at the Prince Cyril Zulu Communicable Diseases Clinic in Durban, South Africa for use in this pathogenesis study while strain E was isolated by Maleka and coworkers in 1996 in our laboratory from a male patient presenting at the same clinic with urethritis.

HaCaT cells were cultured in tissue culture flasks and passaged as described in 3.1.2 and 3.1.3. One day before infection chlamydia growth media medium (CGM) was prepared. The medium consisted of the following: RPMI-1640 supplemented with glucose (5.4 mg/ml), 10 % FBS, 10 mM HEPES, 2mM L-glutamine, gentamicin (10 µg / ml) and amphotericin-B (5 µg / ml).

Once the cells reached 80% confluency, old media were removed, the monolayers were washed with PBS and CGM was added to each flask. Chlamydia EB suspension in sucrose-phosphate-glutamate (SPG) was added to each flask, excluding the negative control to which only SPG was added. Immediately after the inocula had been added the flasks were centrifuged for 1 hour at 1200 x g at 37ºC and incubated for 1 hour at 37°C in 5% CO_2. The media was decanted and replaced with fresh media. The cultures were incubated for a further 2 days at 37°C in 5% CO_2.

After this incubation step, chlamydial inclusions were observed using an inverted phase contrast microscope. For harvesting of chlamydia, the medium was discarded and SPG supplemented with 10% FBS was added to each flask. After addition of 8 to 10 sterile glass beads the flasks were vortexed. The EB-SPG suspension so obtained was transferred to a centrifuge tube which was then centrifuged at 200 x g at 4°C for 10

minutes to pellet cell debris. The supernatant containing chlamydial particles was transferred to a fresh tube and aliquoted into cryovials which were labelled with the isolate number and date and stored at -80 °C.

3.3 Quantification of chlamydia

EB suspensions of each strain were thawed and seven 10-fold serial dilutions were prepared in SPG. These were used to infect 80% confluent HaCaT cell monolayers in a 96-well plate using the infection procedure described in 3.2. After 48 hours incubation, the monolayers were stained as described in paragraph 3.4 and viewed with a fluorescent microscope at 100 x magnification to detect chlamydial inclusion bodies (Joubert 2010). The number of chlamydial inclusions per field of view was counted. The chlamydial infectivity was determined using the following formula:

IFU / ml = $\frac{inclusions}{n}$ x $\frac{1000\mu l}{v}$ x C x D

Where: IFU = Inclusion Forming Unit

n = number of fields counted

V = volume of inoculum (µl)

C = objective lens conversion factor

D = dilution (ml)

3.4 Immunofluorescence staining and microscopy

Cultures were stained using the MicroTrak® *C. trachomatis* Culture Confirmation Test Kit (Trinity Biotech). This staining kit contains anti-*C. trachomatis* monoclonal antibodies raised against the major outer membrane protein (MOMP) present in all 15 known human serovars of *C. trachomatis* and in both EBs and RBs. These monoclonal

antibodies are labelled with fluorescein isothiocynate (FITC) to facilitate species-specific identification of the organism when present in a monolayer of cultured cells, causing chlamydial inclusions to fluoresce apple green in contrast to the host cells which are stained red due to the Evan's blue counter stain.

Immuno-fluorescence staining was performed as follows. Media were carefully aspirated from each well of the 96-well plate. The cell monolayers were immediately covered with 95% ethanol for 5 minutes to fix. Ethanol was aspirated and the monolayers were washed with PBS to remove remaining ethanol.

Following fixation, 15 µl of the stain solution was added to cover the entire monolayer. The plate was covered with a damp gauze pad to create a humidified environment and prevent evaporation during incubation. The plate was incubated for 30 minutes at 37ºC, 5% CO_2 and was agitated every 10 minutes to assure even distribution of the reagent during incubation. Excess reagent was aspirated and the stained monolayers were washed with distilled water. Excess water was removed by gentle tipping the inverted plate on a paper towel covered surface. Plates were then turned back in the upright position and left to air-dry.

The plate was viewed upside down (otherwise the objective could not get close enough) using a fluorescent microscope (Leica DM300) at an excitation/emission peak of 495/517 nm. Chlamydial inclusions appeared apple green in contrast to the host cells, which were stained red.

3.5 Gene expression studies

3.5.1 Study design

The cells that were to be incubated at 37ºC and 33ºC for 2 or 12 hours were infected at an MOI of 100 while the cells that were to be incubated at 37ºC and 33ºC for longer periods were infected at an MOI of 10. We used the lowest MOI which allowed the 16S rRNA real-time PCR to produce a positive result. A low MOI is thought to be more in keeping with the *in vivo* situation however we needed to increase the MOI to 100 for the earlier time points before the organism had begun to replicate. Expression of six chlamydial genes was quantified using real-time PCR and 16S rRNA was used as the reference gene.

3.5.2. Cell culture and infection with *C. trachomatis*

HaCaT cells were seeded into five 12-well plates (2×10^6 cells per well) and incubated at 37°C until the monolayer was approximately 80% confluent. Two of the 12 wells were trypsinized and cell counts were performed (see 3.1.3 and 3.1.5) to calculate the chlamydial inoculum to produce the required MOI. The cell culture media (CCM) was aspirated, the monolayers were washed with PBS to remove unattached dead cells and 1 ml of chlamydia growth medium (CGM) was added to each well. The cells were infected with 100 µl of chlamydial suspension with the required concentration. For the negative control, 100 µl of sterile SPG buffer was added to the relevant wells. The cells were centrifuged at 1200 x g for 1 hour followed by incubation for 1 hour at 33°C or 37°C. The media was then removed and replaced with 2 ml of fresh CGM. Cells were incubated at 33°C or 37°C.

3.5.3. Cell lysis

At 2, 12, 24, 36 and 48 h post infection for experiments at 37°C and at 2, 12, 24, 36, 48, 60 and 72 h post infection for experiments at 33°C, media was removed from the wells and discarded. Two millilitres of guanidine thiocyanate (GTC) solution containing 1.4 % β-mercapto-ethanol (Sigma, Steinheim, Germany) was added per well. This was pipetted up and down multiple times in order to lyse the cells. The cell lysate from each well was transferred to a 15 ml centrifuge tube and the contents of each tube was mixed on a vortex mixer for 2 min. The tubes were then centrifuged at 3000 x g for 30 minutes at 4^{o}C to pellet the chlamydia. The supernatant was decanted and the pellet was re-suspended in 200 µl of GTC solution. This suspension was transferred to a microcentrifuge tube. These tubes were centrifuged at 13000 x g for 20 seconds at 4^{o}C. The supernatant was discarded and the pellet was re-suspended in 200 µl Trisure (Bioline). The chlamydia lysate was transferred to a screw cap microcentrifuge tube with 0.1 mm silicon microbeads (Biospec). The lysate was vortexed for 1 minute and immediately placed on ice for 2 minutes; this step was repeated three times. The microcentrifuge tubes were then stored at -80°C until RNA isolation.

3.5.4 RNA isolation

The microcentrifuge tubes containing chlamydia lysate were retrieved from the freezer and transferred to an icebox. The suspension was centrifuged at 12000 x g for 10 minutes at 4^{o}C. The supernatants were transferred to sterile 2 ml microcentrifuge tubes, which were then allowed to stand at room temperature for 10 minutes. Forty µl cold chloroform (Sigma, Steinheim, Germany) was added. The tubes were vigorously mixed

by shaking manually for 30 seconds. This was followed by incubation at room temperature for 10 min, followed by centrifugation at 12000 x g for 15 minutes at 4^{o}C. The yellowish upper aqueous phase containing RNA was transferred to a sterile 2 ml tube. Hundred µl cold isopropanol (Sigma, Steinheim, Germany) was added to each tube and the contents of the tubes was mixed by inverting three times. The mixtures were then incubated at room temperature for 15 minutes followed by centrifugation at 12000 x g for 15 minutes at 4^{o}C. The supernatant was carefully aspirated without disturbing the gel-like RNA pellet. The RNA was washed by re-suspending the pellet in 200 µl 75% ethanol prepared in diethyl-pyrocarbonate (DEPC)-treated distilled water and this was centrifuged at 7500 x g for 5 minutes at 4^{o}C. The supernatant was carefully decanted and the pellet was air-dried for 10 minutes. The RNA was then re-suspended in 14 µl of RNA-secure using a pipette (10 cycles of aspiration and release). The tubes containing RNA were then incubated for 10 min at 60^{o}C in a water bath and then placed on ice. Quantity and purity of the RNA was measured at 260 nm and 280 nm (260/280) using a NanoDrop 2000C spectrophotometer (Thermo Scientific). Thereafter, based on the absorbance readings, DNase treatment was performed according to manufacturer's instructions to purify the RNA. Quantity and purity of the RNA was measured again. The quality of the purified RNA was confirmed using agarose gel electrophoresis (3.5.4). RNA was stored at -70^{o}C until cDNA synthesis. If cDNA synthesis took place more than one day after RNA isolation, the quality of the RNA was confirmed again using agarose gel electrophoresis to check for deterioration.

3.5.5. Agarose gel electrophoresis

The casting tray, combs and rigs were wiped with 70% ethanol and the open ends of the casting tray was closed with masking tape. A 2% agarose gel was prepared by

dissolving 4 g of agarose (Seakem®LE Agarose, Lonza) in 200 ml Tris-acetate-EDTA (TAE) buffer (1x) (Thermo Scientific). The mixture was allowed to cool till approximately 45ºC and then poured into a casting tray. A comb was inserted and the gel was allowed to solidify (approximately 30 minutes). The comb and masking tape were removed and the casting tray containing the gel was then placed in an electrophoresis tank. TAE buffer (1x) was added until the gel was covered (approximately 500 ml). Ten µl of isolated and purified RNA to be tested was mixed with 3 µl loading dye (containing gel red stain) on a clean piece of Parafilm™. Each mixture was loaded into a well of the gel. The samples were electrophoresed at 100 V for 1 hr. The RNA bands were visualized immediately under UV light.

3.5.6. cDNA synthesis

To synthesize single-stranded cDNA from total RNA, the high capacity cDNA reverse transcription (RT) kit (Applied Biosystems, Life Technologies) was used according to manufacturer's instructions. Thawed RNA was quantified using a NanoDrop 2000C spectrophotometer (Thermo Scientific) and adjusted to 0.2 µg / µl. The kit components were allowed to thaw on ice. The 2x RT master mix was then prepared on ice as shown in table 3.1.

Table 3.1: Components used to prepare a 2x RT master mix

Component	**Volume per reaction tube (20 µl reaction)**
10x RT buffer, 1,0 ml	2.0 µl
25x dNTP Mix (100 mM)	0.8 µl
10x Random Primers, 1.0 ml	2.0 µl
Multiscribe Reverse Transcriptase, 50 U/µl	1.0 µl

RNase Inhibitor	1.0 µl
Nuclease free water	3.2 µl

The cDNA reactions were prepared by pipetting 10 µl of 2 x RT master mix and 10 µl of RNA sample into a 0.2 ml PCR tube. The tubes were sealed and centrifuged briefly to make sure that all fluid was at the bottom of the tube. The tubes were then loaded in the thermal cycler (Gene Amp® PCR System 9700, Applied Biosystems). After the RT PCR was complete, the cDNA was quantified by measuring the absorbance at 260 nm and 280 nm using the Nanodrop spectrophotometer. The cDNA was stored at 2 - 8°C for further use.

3.5.7. Quantitative real-time PCR

Custom Taqman® gene expression assays are gene-specific versions of predesigned real-time PCR 5' nuclease Taqman® assays for relative quantification of gene expression. The custom assays for *groEl-1, incB, pyk-F, tal, omcB* and *hctA* were designed and synthesized by Applied Biosystems (ABI). The 16S rRNA gene was used as reference gene. The sequences (forward primer: 5'TCGAGAATCTTTCGCAATGGAC; reverse primer: 5'CGCCCTTTACGCCCAATAAA; probe: FAM-AAGTCTGACGAAGCGACGCCGC) were obtained from Goldschmidt *et al*., 2006. Primers and probe for this gene were also synthesized by ABI. The PCR reactions were carried out in a final volume of 25 µl as shown in table 3.2.

Table 3.2: Components used to prepare QRT-PCR reactions

Component	**Volume per 25 µl reaction**
Gene expression master mix (Applied Biosystems)	12.5 µl
Custom assay mix 16SrRNA only: Forward primer (0.5 µmol/l) Reverse primer (0.5 µmol/l) FAM-TAMRA Probe (0.4 µmol/l)	1.25 µl 0.25 µl 0.25 µl 0.2 µl
Nuclease free water	8.25 µl
Sample (cDNA eluted in nuclease free water)	2.5 µl

MicroAmp® Optical 96-well Reaction Plates (Applied Biosytems) were used for the PCR reactions. The plates were centrifuged (250 x g, 20 minutes and 24°C) before performing RT-PCR. The amplification and detection was carried out using the ABI Prism 7500 Real -Time PCR System (Applied Biosystems). The PCR cycling programme consisted of 50 two-step cycles of 15 sec at 95°C, and 1 minute at 60°C. Data were presented as the mean cDNA copy number obtained for each gene divided by the corresponding mean 16S rRNA values. Relative fold change was calculated using the comparative $2^{-\Delta\Delta CT}$ method.

3.6 Transmission Electron Microscopy (TEM)

Transmission electron microscopy was performed at the same time points and temperatures used in the gene expression experiments to confirm the stage of the developmental cycle that the organism was at inside the keratinocytes at each of these time points. The results of the gene expression assays were compared with transmission electron microscopy done under the same.

3.6.1 Monolayer preparation and infection

HaCaT cells were grown in tissue culture flasks. Confluent cells were trypsinised (3.1.3) and 1 x 10^5 cells seeded in each well of a 24 well tissue culture plate containing Thermanox coverslips (Nunc) with a diameter of 12 mm. When cells were approximately 90% confluent, cells were trypsinized and enumerated (3.1.3 and 3.1.5). The residual CCM was aspirated and the monolayer was washed once with PBS. Following this, chlamydial growth medium was added. The chlamydial inoculum was thawed and diluted to the required concentration with SPG buffer, and inoculated onto cells. The cells that were to be incubated at 37ºC and 33ºC for 2 or 12 hours were infected at an MOI of 100 while the cells that were to be incubated at 37ºC and 33ºC longer were infected at an MOI of 10. For the negative control, 100 µl sterile SPG buffer without chlamydia was added. Cells were centrifuged immediately at 1200 x g for 1 hour at 37ºC and then incubated at 37ºC in 5% CO_2. The SPG buffer with the residual inoculum was removed after 2 hours of incubation and replaced with 1 ml fresh CGM.

3.6.2 Monolayer processing

At each time point, one monolayer infected with each strain at each of the incubation temperatures was fixed and processed for transmission electron microscopy (TEM). After washing with EMEM, the coverslips with infected monolayers were transferred to a dry sterile 24- well plate using sterile forceps and a dissecting needle. The original plate was returned to the incubator, while the harvested coverslips with their cell monolayers were processed within the 24-well plate to which they had been transferred.

Cells were fixed with 2% gluteraldehyde in EMEM for 30 minutes, and then washed with EMEM twice for 5 minutes. The fixed monolayers were covered by a layer of sterile EMEM and refrigerated until further processing (no more than 20 hours). The preparation process is summarized in table 3.3. In order to embed the fixed cells for TEM, a beam capsule was filled with Spurr resin and the coverslip placed on top of the beam capsule with the cell-side down and in contact with the resin. This structure was incubated at 60°C for 8 hours to allow the resin to solidify. After 8 hours the coverslip was removed.

Table 3.3 Processing schedule for TEM

Step	Process	Solution	Temperature	Time
1	Fixation	2% gluteraldehyde in EMEM	24ºC	30 min
2	Wash	EMEM	24ºC	5 min
3	Wash	EMEM	24ºC	5 min
4	Wash	Sodium cacodylate buffer	24ºC	5 min
5	Post- fixation	1% osmium tetroxide[a]	24ºC	1hour
6	Wash	Sodium cacodylate buffer	24ºC	5 min
7	Wash	Sodium cacodylate buffer	24ºC	5 min
8	Dehydration	50% ethanol	24ºC	10 min
9	Dehydration	70% ethanol	24ºC	10 min
10	Dehydration	90% ethanol	24ºC	10 min
11	Dehydration	100% ethanol	24ºC	10 min
12	Dehydration	100% ethanol	24ºC	10 min
13	Dehydration	100% ethanol	24ºC	10 min
14	Infiltration	Ethanol : Spurr resin (1:1)[b]	24ºC	30 min
15	Infiltration	Spurr resin[b]	60ºC	1 hour
16	Infiltration	Spurr resin[b]	60ºC	1 hour
17	Embedding	Spurr resin	60ºC	8 hours

[a] protected from light

[b] procedure carried out uncovered to allow polypropylene to evaporate

3.6.3 Ultramicrotomy

The section of the resin block containing cells was cut and trimmed to produce a "mesa" with a trapezoidal shape. Ultrathin sections (50-60 nm) were cut and collected onto uncoated copper 200 mesh grids, then double stained with uranyl acetate and Reynold's lead citrate for 10 minutes respectively (Young and Elliott 1989). Uranyl acetate and Reynolds lead citrate were decanted and centrifuged to pellet any debris or solute crystals. Grids were floated on a drop of uranyl acetate for 10 minutes, rinsed twice with triple distilled water and blotted dry on a filter paper. They were then placed in a drop of Reynolds lead citrate, rinsed twice with triple distilled water and blotted dry.

3.6.4 Visualization and photography

Sections were viewed using a Jeol 1010 transmission electron microscope at an accelerating voltage of 100 kV. The TEM was interfaced with a Megaview III Software Imaging Systems camera unit. Images were captured digitally and measurements performed using iTEM analySIS (Germany) image analysing software.

CHAPTER 4: RESULTS

4.1 Quantitative real-time PCR

A validation analysis of standard curves for $\Delta\Delta C_T$ method was performed for the six selected *Chlamydia trachomatis* genes. These are *groEL-1*, *incB*, *pyk-F*, *tal*, *hctA* and *omcB*. The ΔC_T values were plotted vs. log input amount cDNA to create a semi-log regression line. The gradients of the regression lines were for *groEL-1* -0.0162, for *incB* 0.0106, for *pyk-F* -0.0011, for *tal* 0.0112, for *hctA* 0.0261 and for *omcB* 0.0417 (Figure1). Since all six values were < 0.1, the analysis is valid for all.

Following the validation analysis, relative quantitation of gene expression was performed and the mean fold difference was calculated using the comparative $2^{-\Delta\Delta CT}$ method (Biosystems 2004). We analyzed the expression of the six *C. trachomatis* genes using total RNA harvested at 2, 12, 24, 36 and 48 hours post infection for cells incubated at 37^{o}C and at 2, 12, 24, 36, 48, 60 and 72 h post infection for cells incubated at 33^{o}C. The summary of the gene expression results is given in table 4.1.

The *groEL-1* and *incB* genes were expressed at every time point at both 37^{o}C and 33^{o}C for strains L2 434, L2 US151 and strain E (fig.2 A-D). At 37^{o}C, the expression levels for *groEL-1* (fig.2A) and *incB* (fig. 2C) were at its highest at 2 hours post infection, and then gradually decreased thereafter for all three strains. The expression levels for L2 434 were considerably higher at 2, 12, 24 and 36 hours post infection compared to L2 US151. Fig. 2B shows the results for *GroEL-1* at 33^{o}C. Like at 37^{o}C, *groEL-1* expression by strain L2 434 was observed at all time points at low levels throughout the developmental cycle. *GroEL-1* expression levels also remained low up till 12 hours

post infection in L2 US151 but with this strain an approximately 10-fold increase was observed from 24 hours post infection onwards. At 33^{o}C expression levels of strain E varied but without a clear trend. At 37^{o}C *incB* expression (fig 2C) was high at 2 hours post infection in strain L2 434 but declined rapidly. Strain L2 US151showed low levels of expression throughout. Expression levels of strain E were high during the first 12 hours post infection but low after that. At 33^{o}C (fig. 2D), *incB* expression levels of L2 434 and US151 remained constant throughout the developmental cycle with a peak at 48 hours for the latter. In strain E, the expression levels peaked at 12 hours post infection, remained high up till 24 hours and decreased thereafter.

At 37^{o}C, *pyk-F* expression levels (fig. 3A) in both LGV strains were highest at 2 hours post infection, then decreased in the period between 2 and 24 hours and remained constantly low from 24 hours post infection. Expression levels of *pyk-F* over time in strain E were similar to the LGV strains but at lower levels. In contract to 37^{o}C, *pyk-F* expression levels at 33^{o}C (fig. 3B) remained low between 2 and 12 hours post infection, and then increased from 24 hours post infection. As expected *pyk-F* was detected from 12 hours post infection with E, but from 24 hours post infection with L2 US151 and throughout the developmental cycle for L2 434. Strain L2 434 had the lowest expression levels at this temperature. *Tal* was also detected throughout the developmental cycle for all three strains at both temperatures (fig 3C and D) but the expression levels differed. *Tal* expression levels remained constantly low throughout the cycle for L2 434 and US151 but were high between 2 and 12 hours post infection for E at 37^{o}C (fig. 3C). At 33^{o}C, *tal* expression was observed at all time points with a gradual increase of expression levels till the peak was reached for all three strains at 48 hours post infection (fig 3D).

At 37°C, *hctA* expression of L2 434 was at its highest level at 2 hours post infection and declined gradually till 48 hours post infection. Although there was a similar expression by strains L2 US151 and E, the values were lower and the decline less outspoken (fig 4A). At 33°C, *hctA* expression (fig 4B) was detected from 12 hours post infection, and then a 2.5-fold increase was observed at 24 hours post infection for L2 434. Expression levels remained constantly low throughout the developmental cycle for L2 US151. *HctA* expression was also detected from 12 hours post infection, and then a 0.5-fold increase was observed at 24 as well as at 72 hours post infection for strain E (fig. 4B). At 37°C, *omcB* expression (fig 4C) was high at 2 hours post infection, levels decreased at 12 hours post infection, and then a 5-fold increase was observed at 24 hours post infection for L2 434. The expression levels remained constantly low throughout the developmental cycle for L2 US151. Expression was high between 2 and 12 hours post infection, and then a 3-fold decrease in expression was observed at 24 hours post infection for E (fig. 4C). At 33°C, high levels of *omcB* expression (fig 4D) were detected from 24 till 48 hours post infection for L2 434, but remained constantly low throughout the developmental cycle for L2 US151 and E.

To verify the observations in HaCaT cells, we performed the same analysis in HeLa cells. Table 4.2 summarizes the results of RT-PCR analysis in infected HeLa cells for three (*groEL-1*, *pyk-F*, *hctA*) chlamydial genes representing each of the three proposed temporal classes of chlamydial gene expression. The results obtained were in keeping with the published research as *groEL-1* was detected from 2 hours post infection, *pyk-F* from 12 hours post infection and *hctA* from 24 hours post infection (Shaw, Dooley et al. 2000).

4.2 Transmission electron microscopy (TEM)

An ultrastructural analysis was performed using TEM to place transcriptional events into context of the *C. trachomatis* biovar LGV and biovar G developmental cycle, and to confirm the stage of the developmental cycle that the organism is in the keratinocytes while expressing the various genes.

EBs were about 200 -300 nm in diameter, with a dark highly condensed inner region. As differentiation of EB to RB occurred, an increase in size was apparent. RBs were about 1 μm in diameter and had a pleomorphic shape.

At 37ºC and 33ºC, both LGV (L2 434 and US151) and G (E) strains presented the normal chlamydial replication cycle comprising EB and RB. The ultrastructural events observed during *C. trachomatis* LGV and G developmental cycle at 37ºC and 33ºC are depicted in figures 5, 6 and 7.

Figure 5 shows the ultrastructural events of strain L2 434 at 37ºC and 33ºC. Figure 5A and B show uninfected HaCaT cells grown at 37ºC and 33ºC respectively, which appeared polygonal in shape and had a centrally located nucleus containing nucleoli. Infected HaCaT cells appeared similar to uninfected cells at 2 hours post infection as there were no noticeable morphological differences and not much was observed within the cells at both temperatures (fig. 5C and D). Strain L2 434 replicated faster at 37ºC than at 33ºC. At 12 hours post infection, there were approximately 26 RBs within the inclusion at 37ºC (fig. 5E) and only four at 33ºC (fig. 5F). As the organisms differentiated into mature RBs, an increase in size was apparent. At 12 hours post

infection RBs reached mature size at both temperatures and showed evidence of binary fission. The inclusions also expanded to accommodate the increasing number of RBs. EBs were first seen at 36 hours post infection at 37ºC (fig. 5I) compared to 48 hours post infection at 33ºC (fig.5 L). At 37ºC, EBs continued to accumulate within the inclusion at 48 hours post infection (fig. 5K). At 33ºC, the inclusion looked ruptured as there was no definite distinct division between the cytoplasm of the host cell and the inclusion matrix at 60 and 72 hours post infection (fig. 5M and N), and fewer EBs were still within the inclusion matrix.

Strain L2 US151 (fig. 6) showed similar ultrastructural events as strain L2 434, except that at 2 hours post infection at both temperatures (fig. 6C and D) at least one organism was seen within the cell, although no increase in size or replication was yet apparent. Furthermore, at 60 hours post infection (fig. 6M) a mixture of numerous RBs and EBs were still compartmentalized within the inclusion.

Figure 7 shows the ultrastructural events of strain E at 37ºC and 33ºC. Figure 7 A and B show uninfected cells. Similar to strain L2 434, not much was observed at 2 hours post infection at both temperatures (fig. 7 C and D). However, at 33ºC a new immature inclusion was beginning to from at 12 hours post infection (fig. 7F) compared to 37ºC where the inclusion was already formed and had approximately 7 mature RBs (fig. 7E). Similar to strains L2 434 and US151, EBs were first seen at 36 hours post infection at 37ºC (fig. 7I) compared to 48 hours post infection at 33ºC (fig. 7L). In contrast to strain L2 434, a mixture of RBs and EBs were still compartmentalized within the inclusions at 60 and 72 hours post infection (fig. 7M and N)

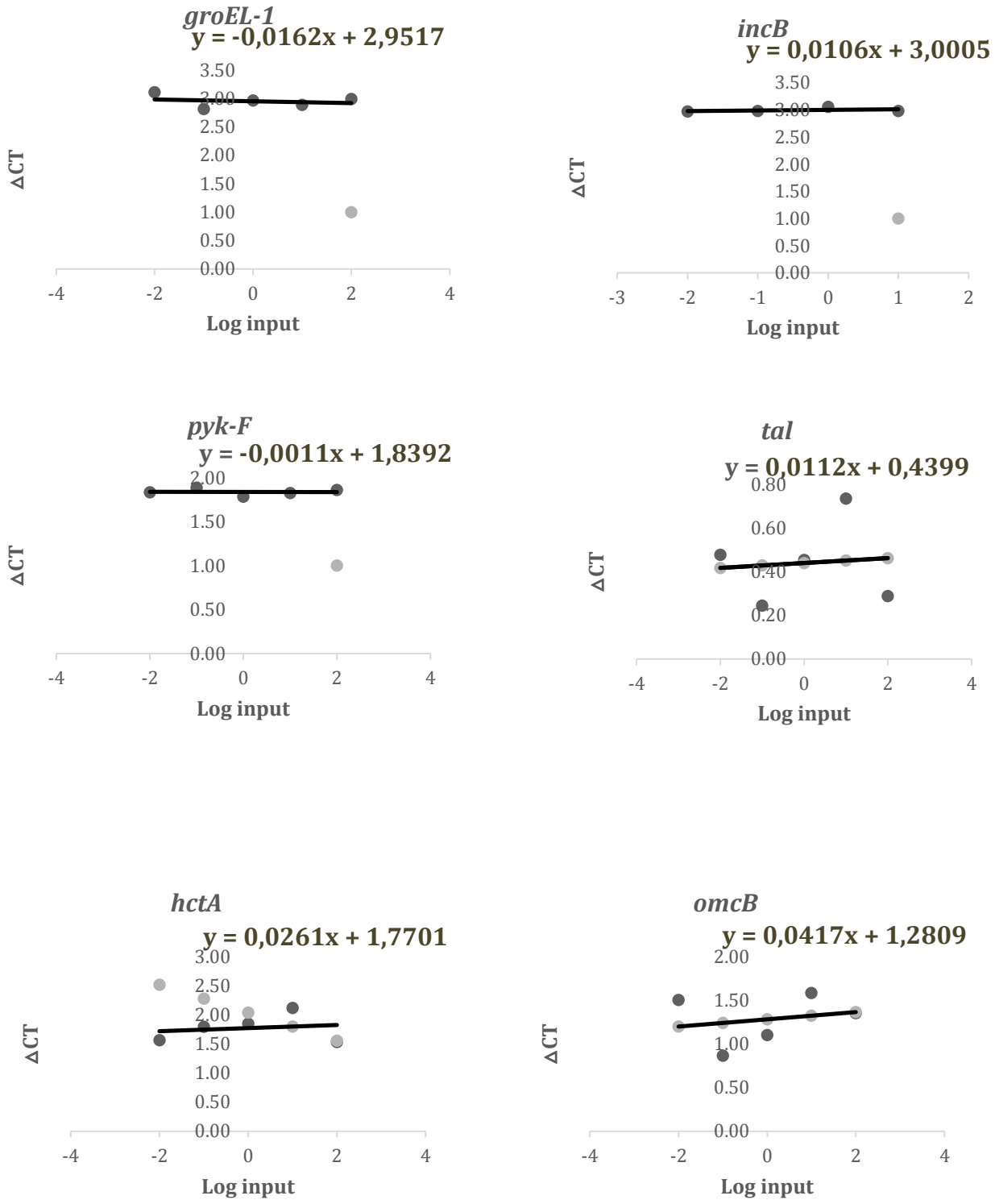

Figure 1: Validation analysis of chlamydial gene standard curves for $\Delta\Delta C_T$ method

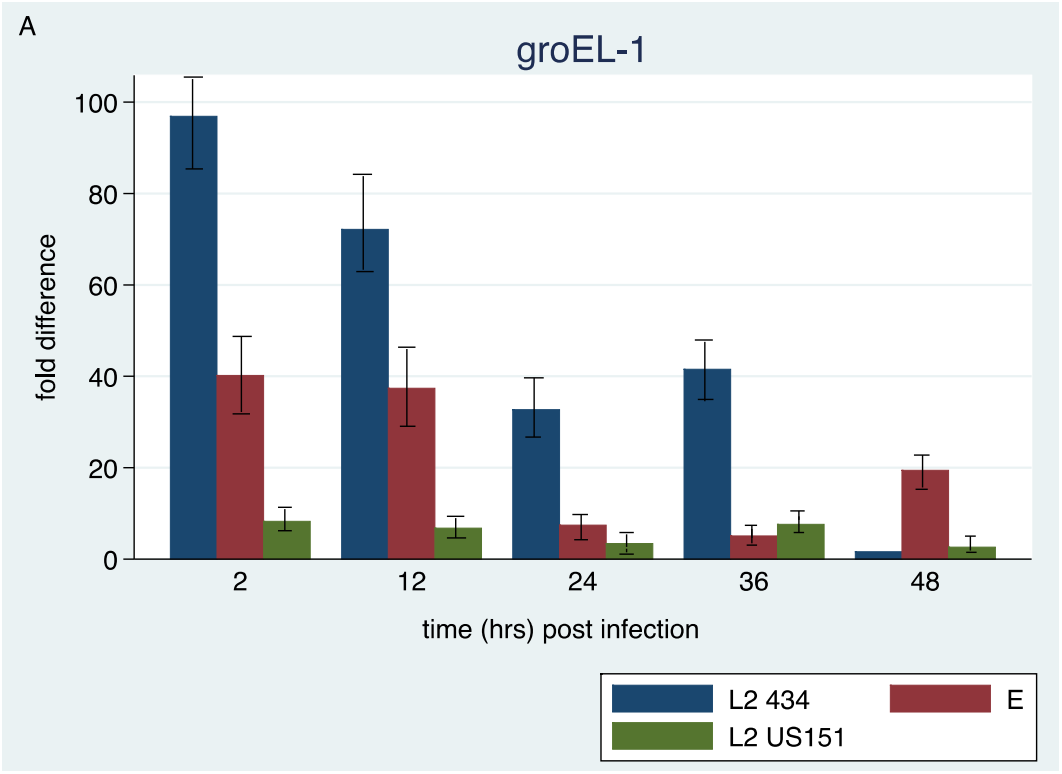
A
groEL-1
fold difference
0
20
40
60
80
100
2
12
24
36
48
time (hrs) post infection
L2 434
E
L2 US151

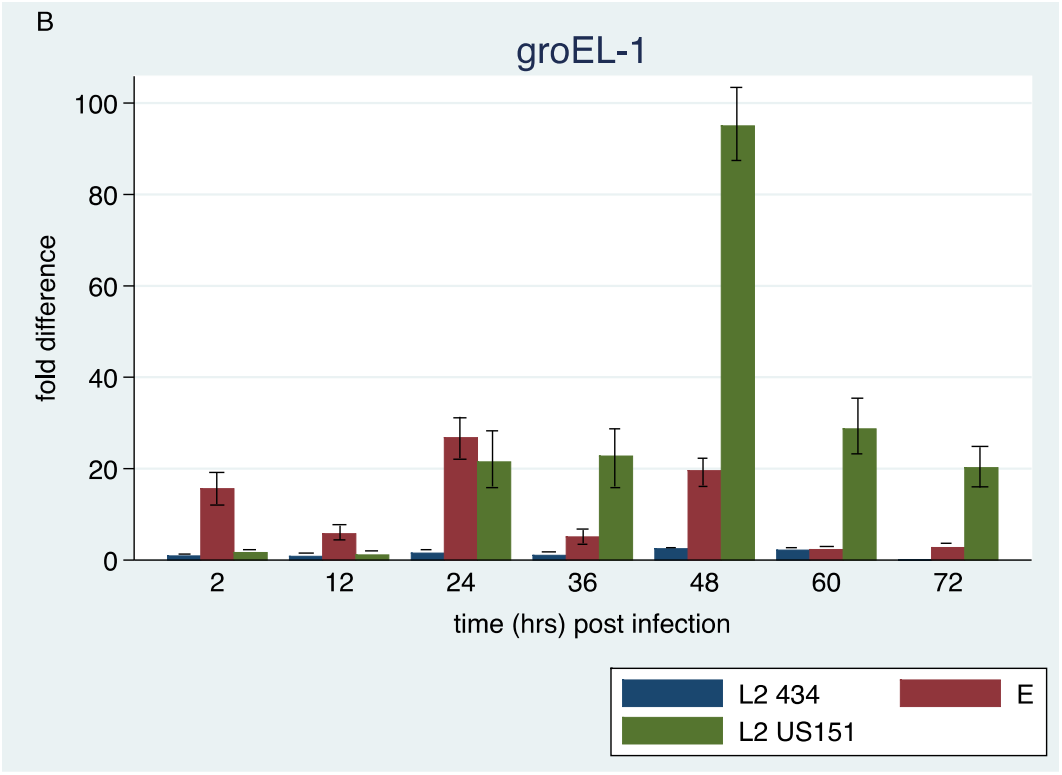
B
groEL-1
fold difference
0
20
40
60
80
100
2
12
24
36
48
60
72
time (hrs) post infection
L2 434
E
L2 US151

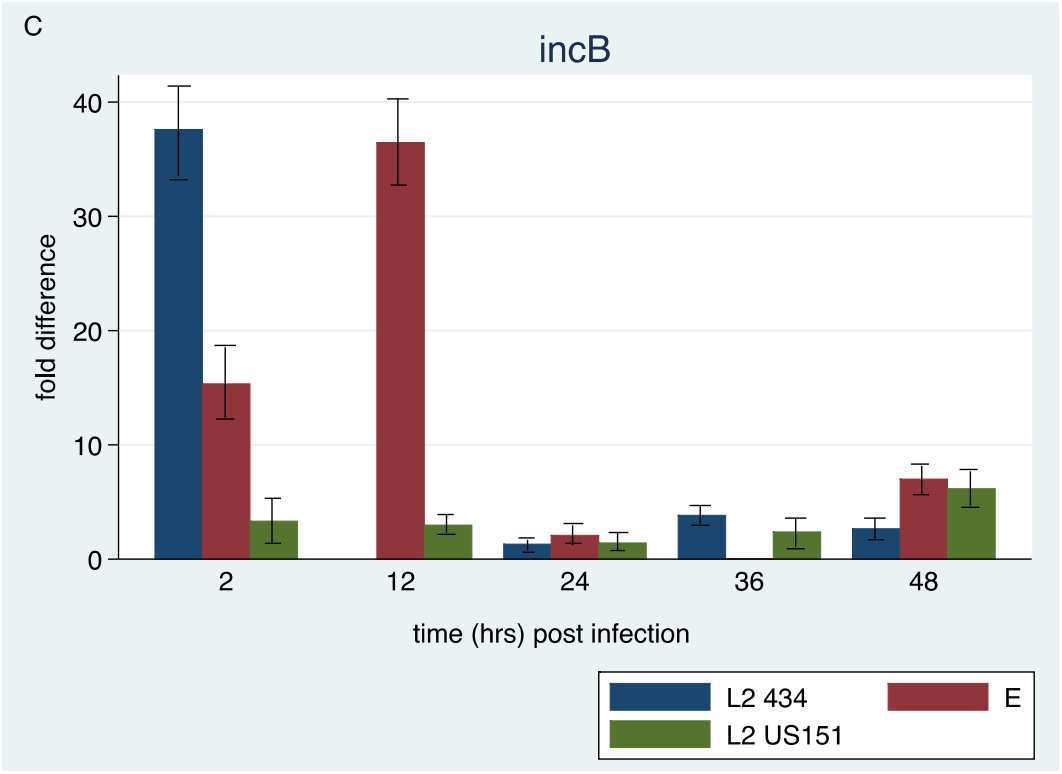

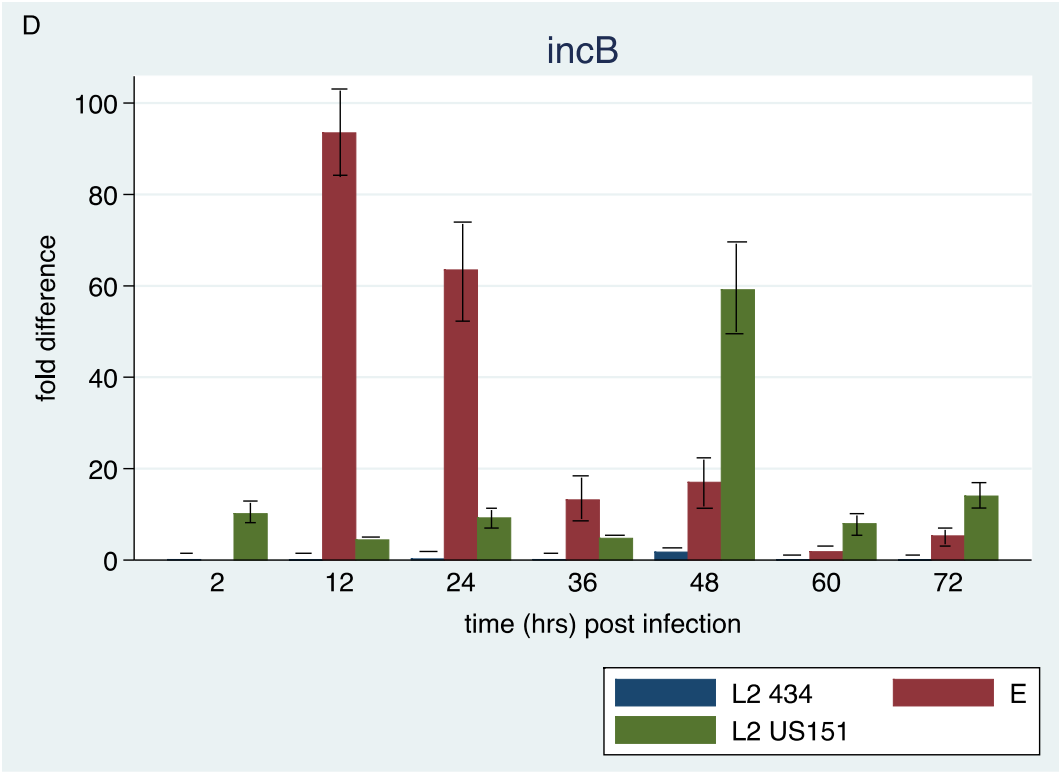

Figure 2: Expression levels of early-cycle genes at 37ºC (A, C) and 33ºC (B, D) detected by quantitative RT-PCR. Values represent the mean fold difference ($2^{-\Delta\Delta CT}$) and the error bars indicate the standard error of the mean

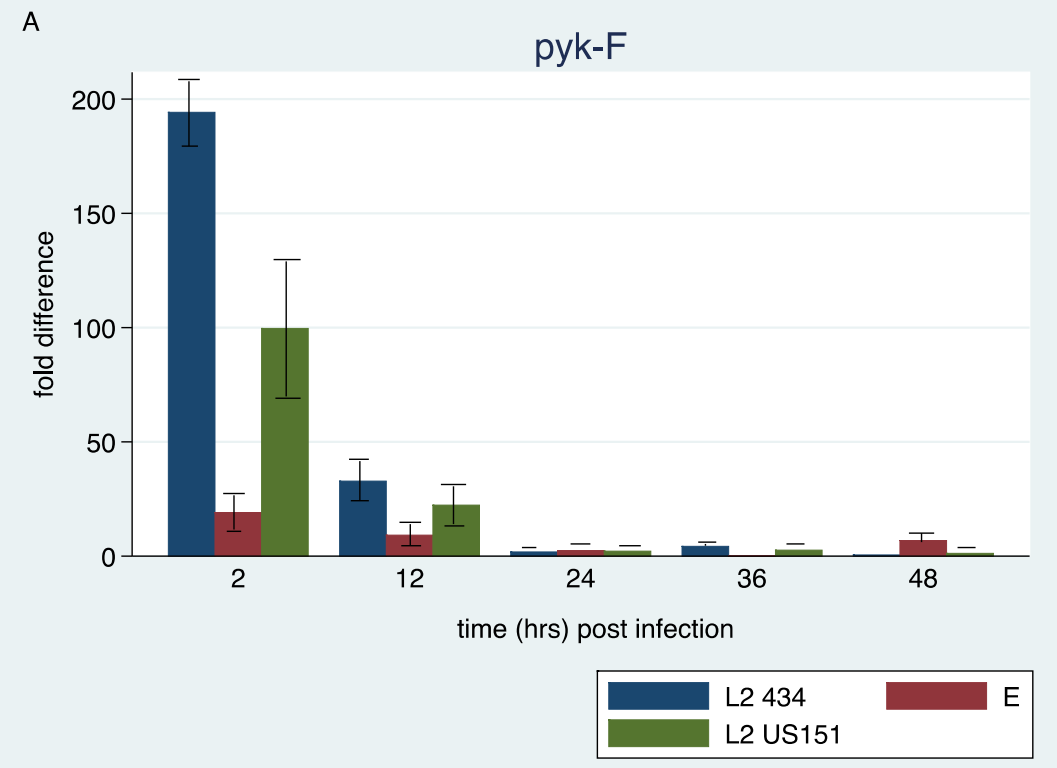
A
pyk-F
200
150
100
50
0
fold difference
2
12
24
36
48
time (hrs) post infection
L2 434
E
L2 US151

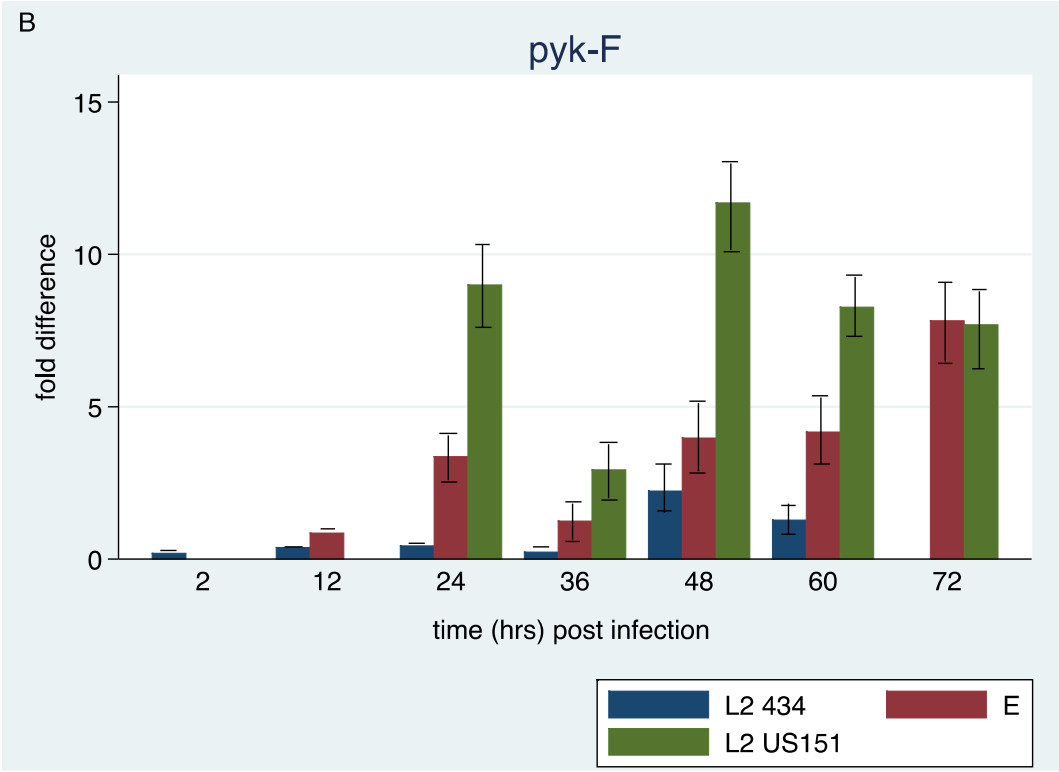
B
pyk-F
15
10
5
0
fold difference
2
12
24
36
48
60
72
time (hrs) post infection
L2 434
E
L2 US151

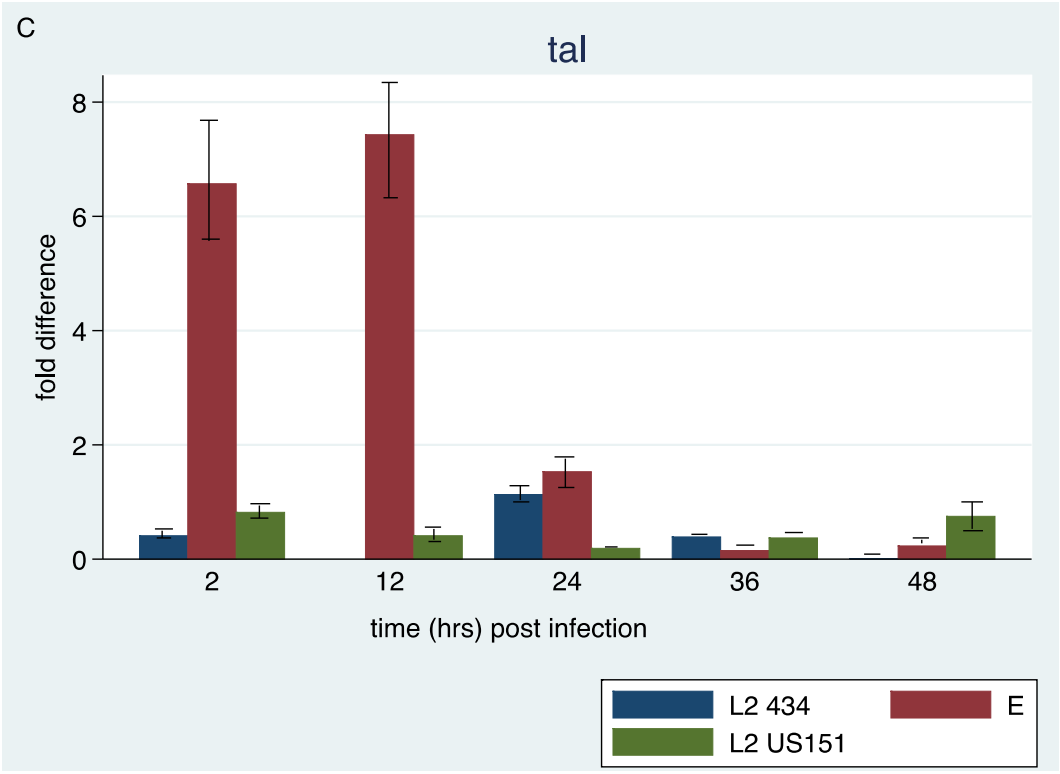

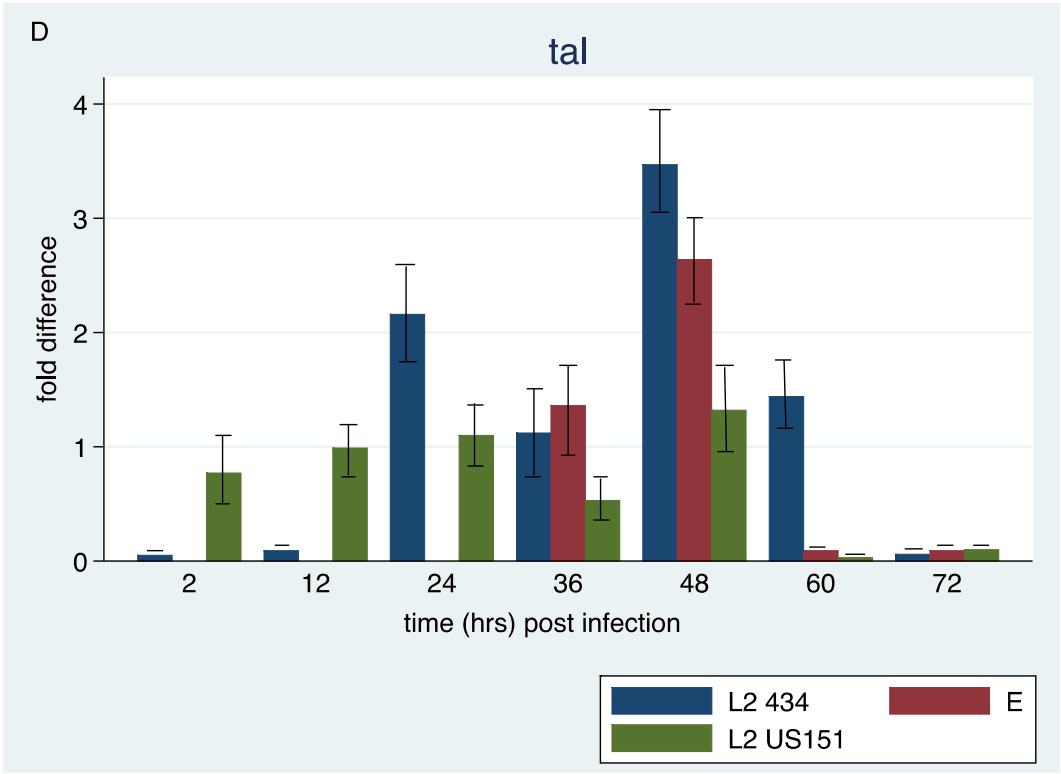

Figure 3: Expression levels of mid-cycle genes at 37°C (A, C) and 33°C (B, D) detected by quantitative RT-PCR. Values represent the mean fold difference ($2^{-\Delta\Delta CT}$) and the error bars indicate the standard error of the mean.

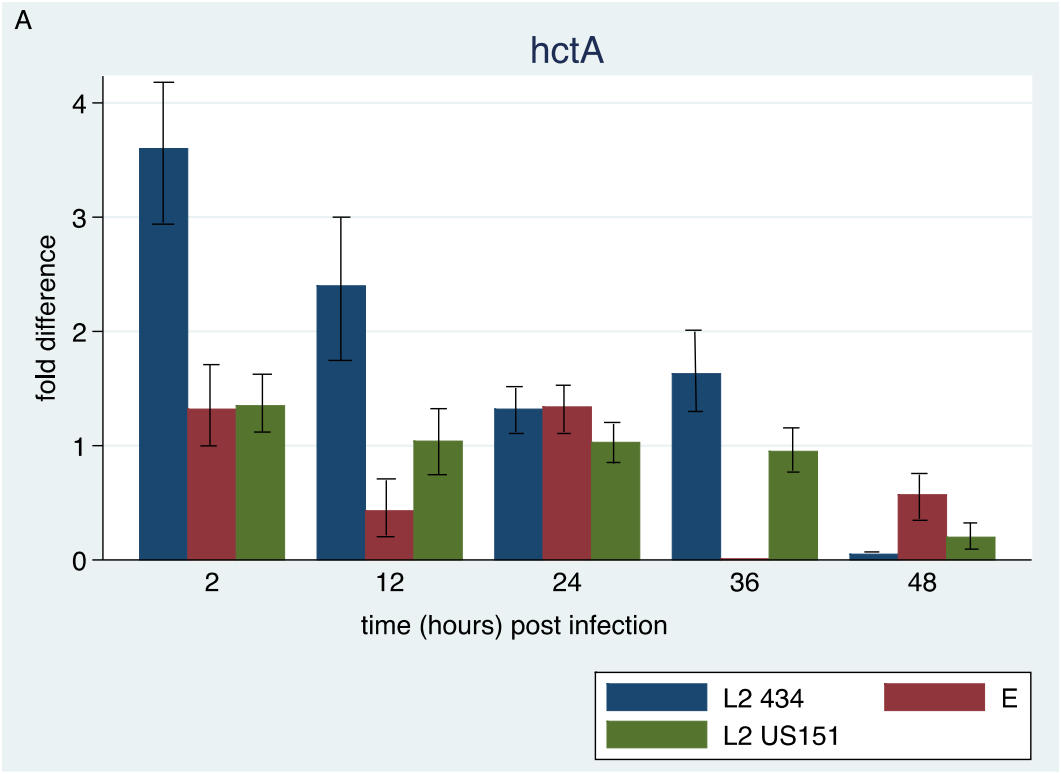
A
hctA
fold difference
0
1
2
3
4
2
12
24
36
48
time (hours) post infection
L2 434
E
L2 US151

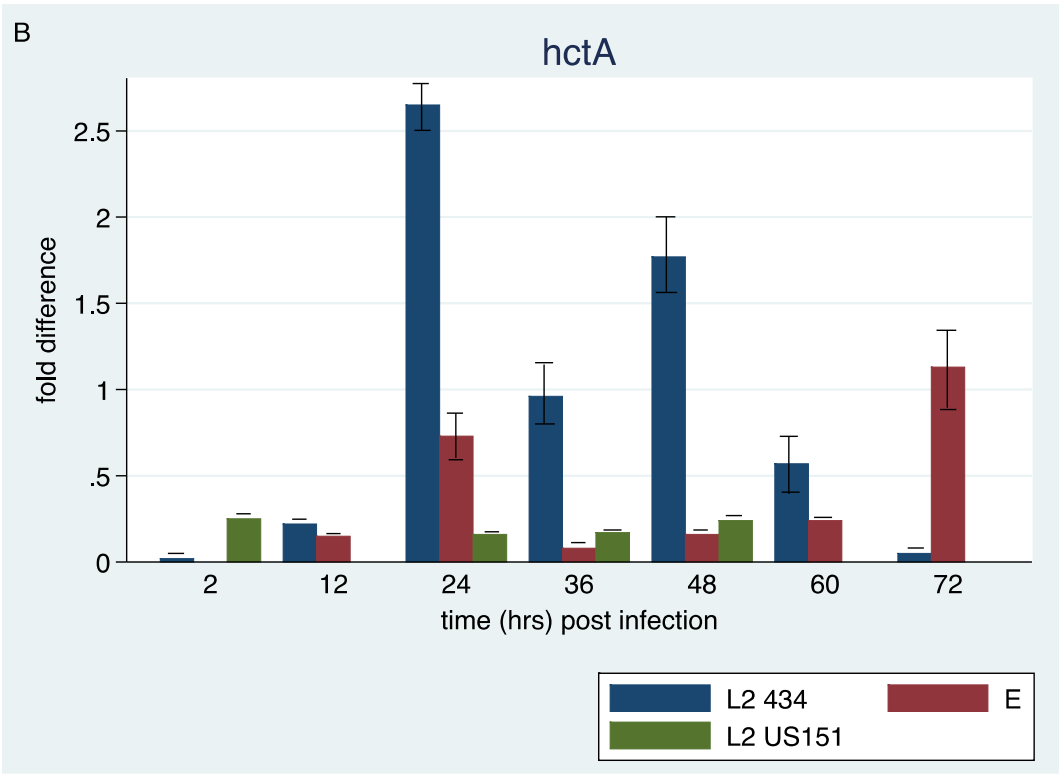
B
hctA
fold difference
0
.5
1
1.5
2
2.5
2
12
24
36
48
60
72
time (hrs) post infection
L2 434
E
L2 US151

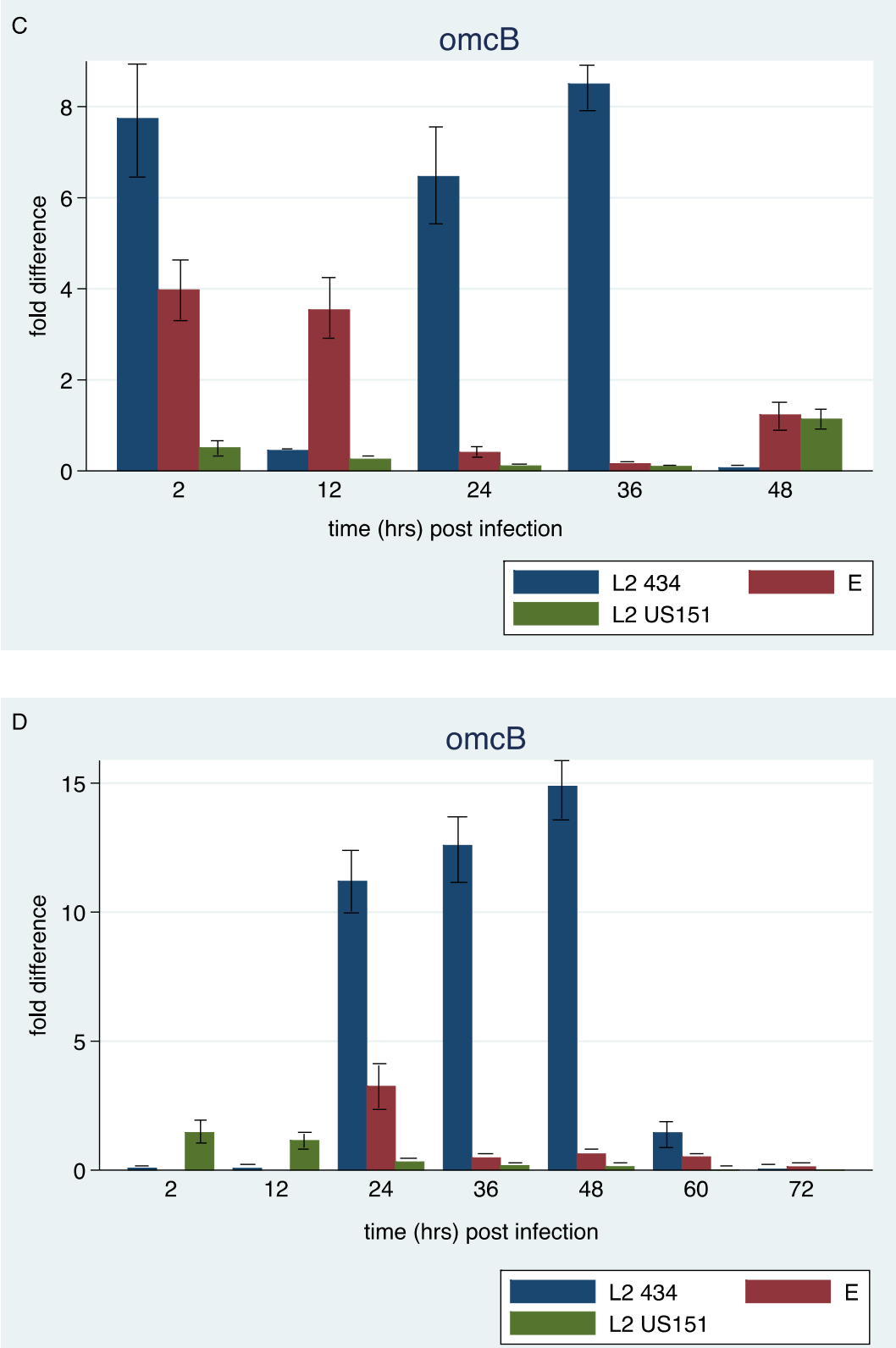

Figure 4: Expression levels of late-cycle genes at 37°C (A, C) and 33°C (B, D) detected by quantitative RT-PCR. Values represent the mean fold difference ($2^{-\Delta\Delta CT}$) and the error bars indicate the standard error of the mean.

Table 4.1: Expression of chlamydial genes in HaCaT cells at 37 ºC and 33ºC

		Expression peak time point (hours post infection)					
		37ºC			33ºC		
Gene	**Function**	**L2 434**	**US151**	**E**	**L2 434**	**US151**	**E**
GroEL-1	**Chaperonin (60 kDa)** – Stabilizes cellular proteins	2 - 12	Continuous expression	2 -12	Continuous expression	48	Continuous expression
IncB	**Inclusion membrane protein** – Mediates interaction between chlamydia and the host cell	2	Continuous expression		Continuous expression	48	12
Pyk-F	**Pyruvate kinase** – Energy metabolism during glycolysis pathway	2	2	2 -12	Continuous expression	24 – 72	24 -72
Tal	**Transaldolase** – Energy metabolism during the pentose phosphate pathway	Continuous expression	Continuous expression	2 -12	24 -60	2 -48	2 -48
HctA	**Histone-like protein** – Condensation of chromosome during the differentiation of ERs to EBs	2 -12	2 -36	2 and 24	24	2 – 48	72
OmcB	**Cysteine-rich OMP (60 kDa)** – Ensures Eb rigidity	2, 24 and 36	Continuous expression	2 – 12	24 – 48	Continuous expression	24

Table 4.2: Temporal expression of selected chlamydial genes in HeLa cells infected with L2 at 37ºC

	Time (hours) post infection				
Gene	2	12	24	36	48
groEL-1	+	+	+	+	+
Pyk-F	-	+	+	+	+
hctA	-	-	+	+	+

+, Amplification detected

-, No amplification detected

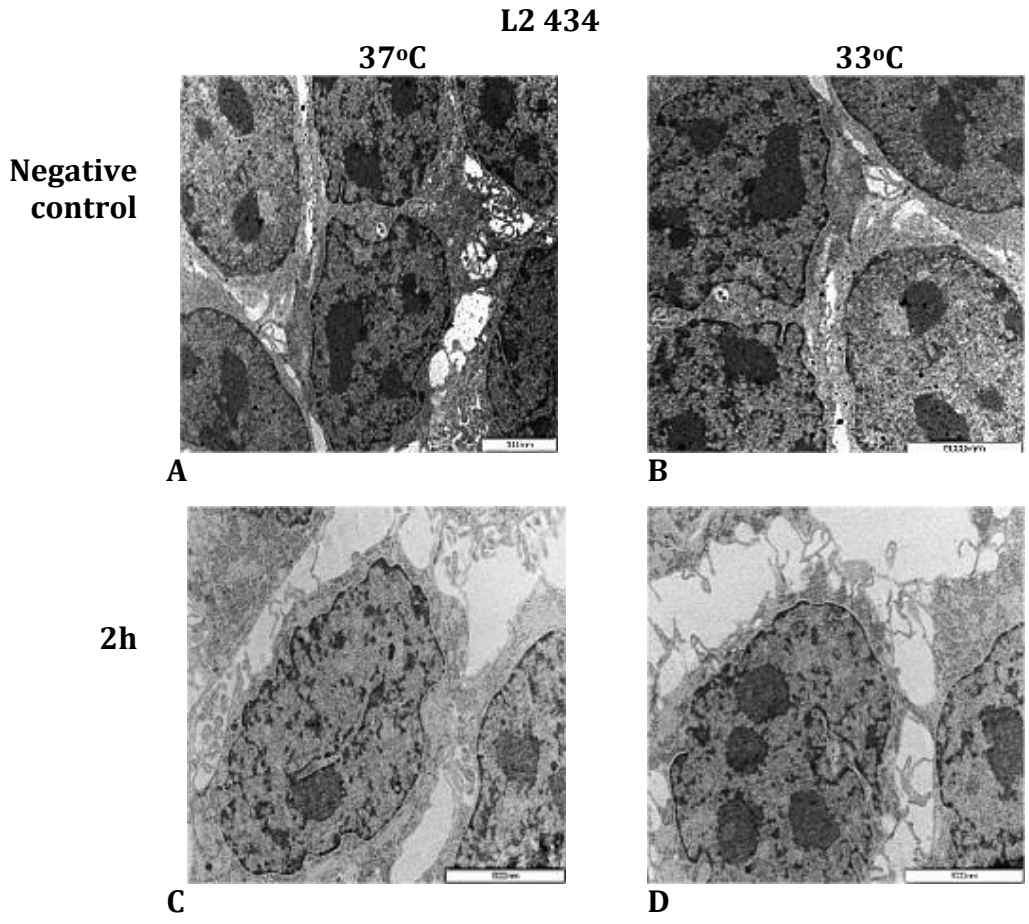

12h

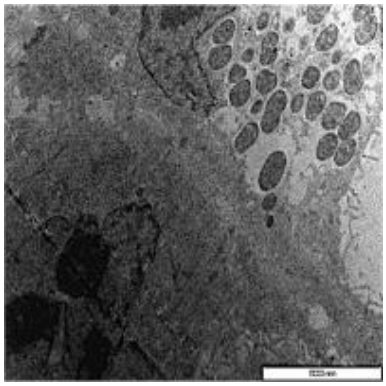

E

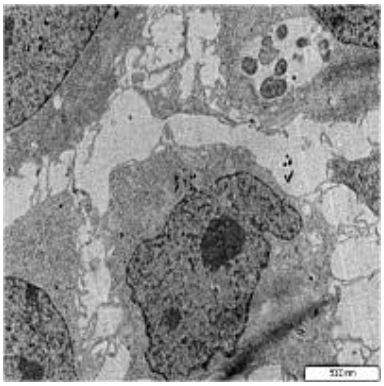

F

24h

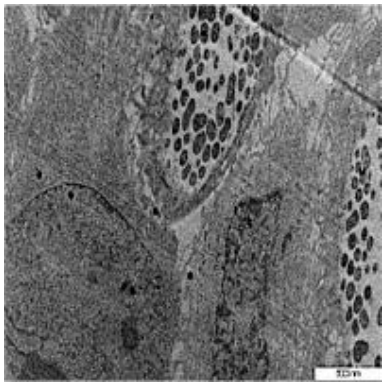

G

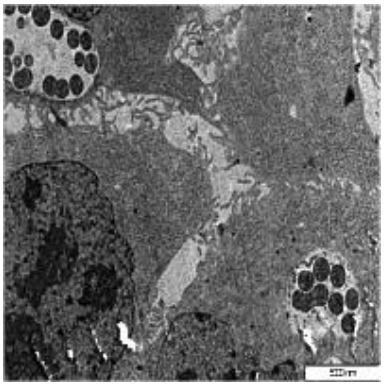

H

36h

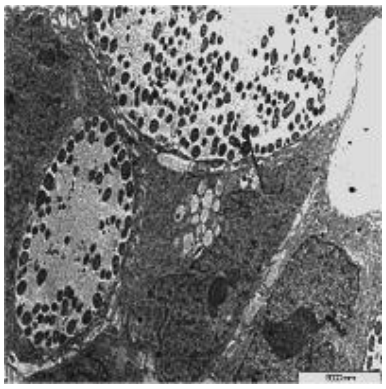

I

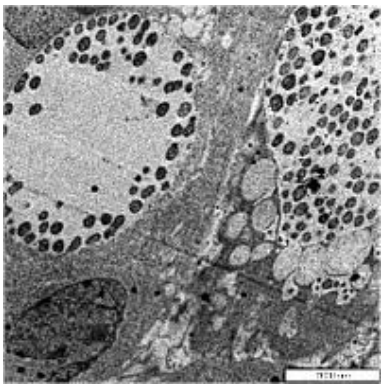

J

48h

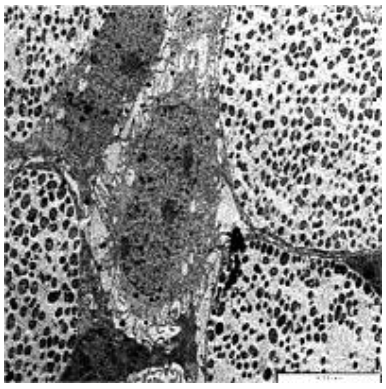

K

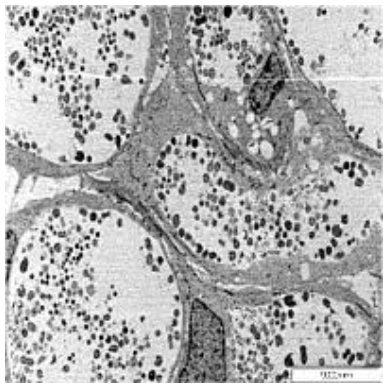

L

60h

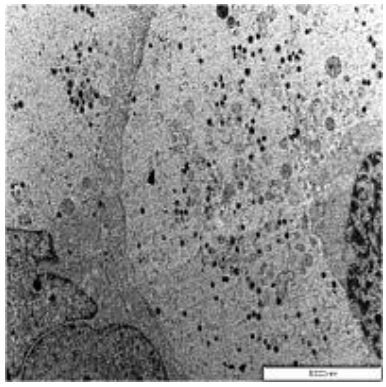

M

72h

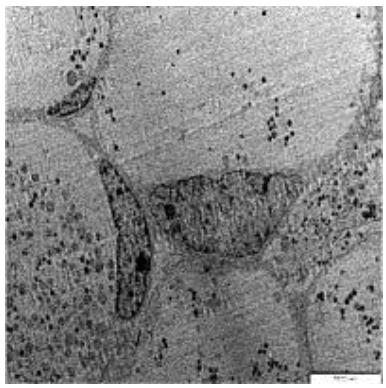

N

Figure 5: TEM micrographs of HaCaT cells infected with *C. trachomatis* L2 434 demonstrating differentiation, growth, division and redifferentiation at 37°C and 33°C over the course of the developmental cycle. Uninfected (A), 2h (C), 12h (E), 24h (G), 36h (I) and 48h (K) post infection at 37°C. Uninfected (B), 2h (D), 12h (F), 24h (H), 36h (J), 48h (L), 60h (M) and 72h (N) Cultures in C-E and D-F were infected at an MOI of 100 to increase the likelihood of visualizing organisms in thin sections. Cultures in G-K and H-N were infected at an MOI of 10. Bar, 500 nm.

L2 US151

37°C **33°C**

Negative control

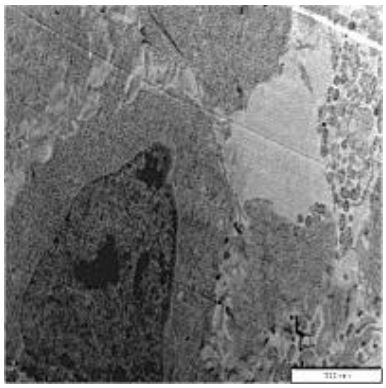

A

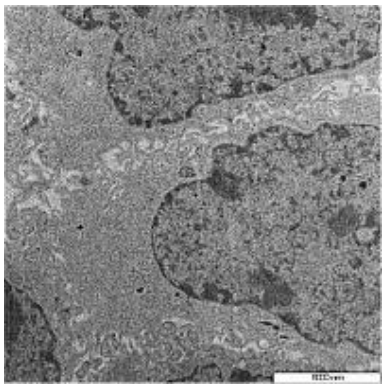

B

2h

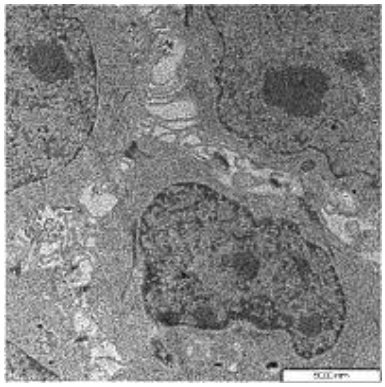

C

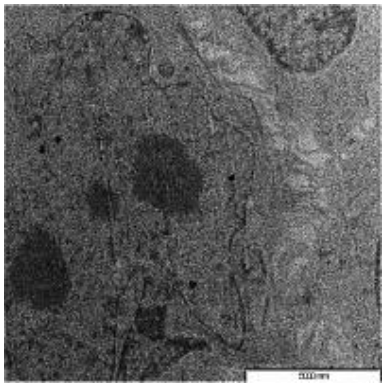

D

12h

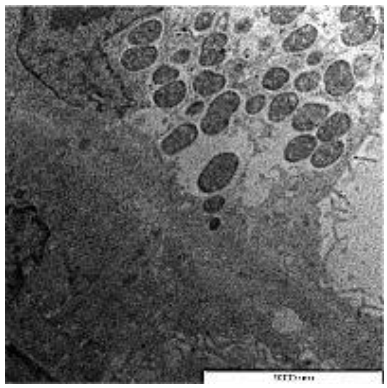

E

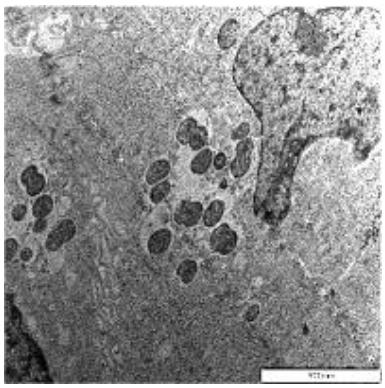

F

24h

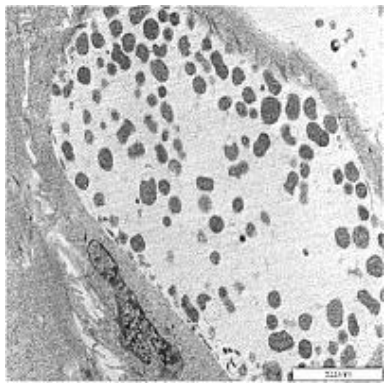

G

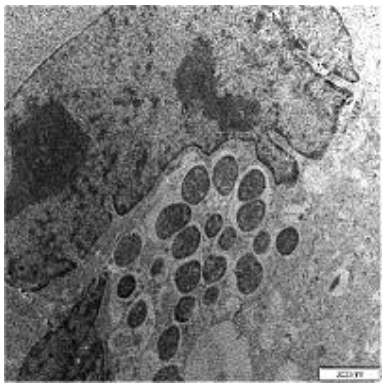

H

36h

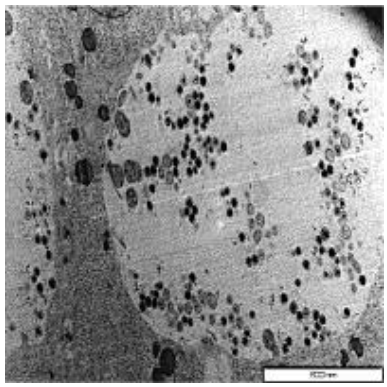

I

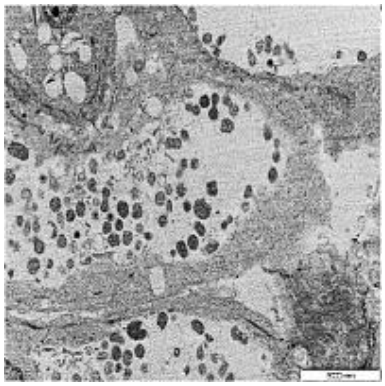

J

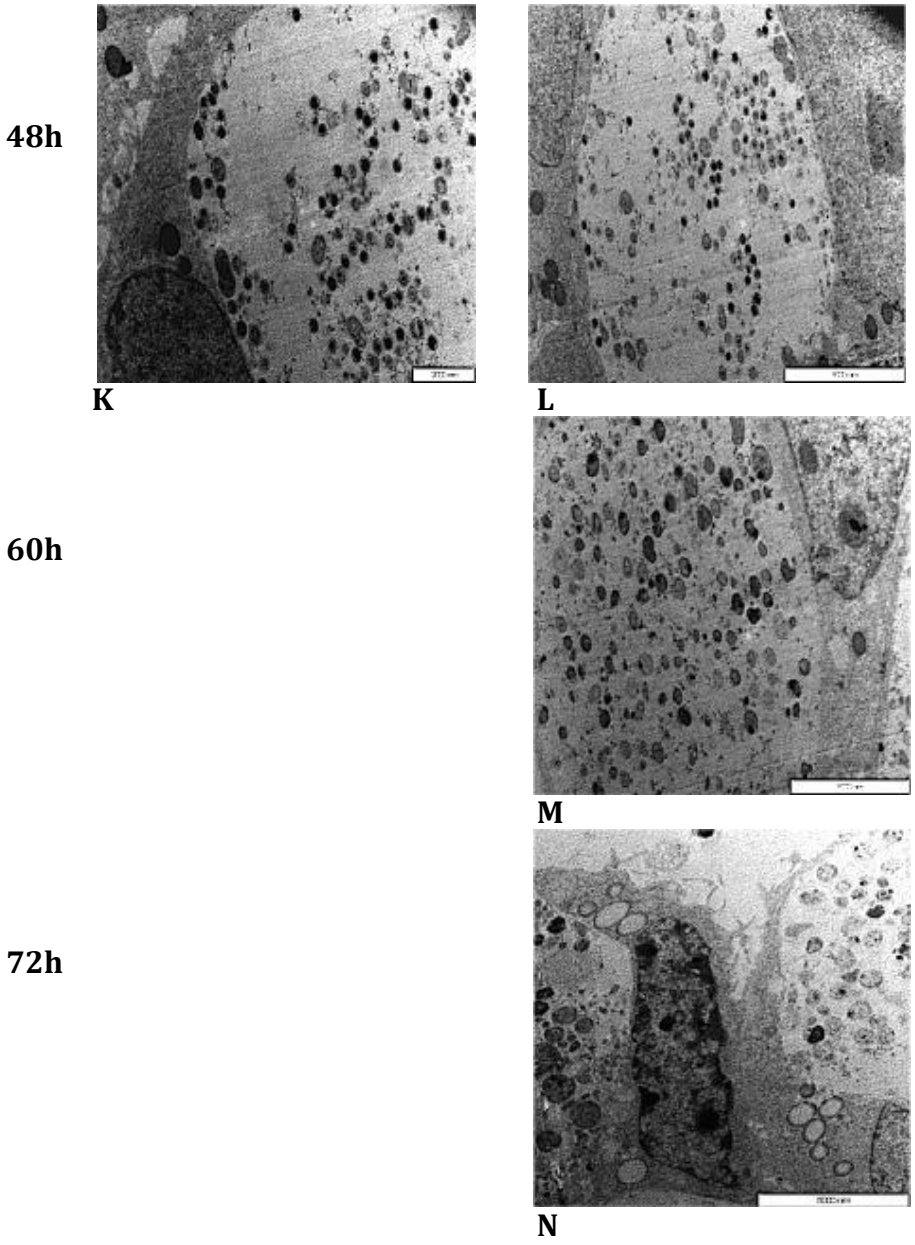

Figure 6: TEM micrographs of HaCaT cells infected with *C. trachomatis* E demonstrating differentiation, growth, division and redifferentiation at 37°C and 33°C over the course of the developmental cycle. Uninfected (A), 2h (C), 12h (E), 24h (G), 36h (I) and 48h (K) post infection at 37°C. Uninfected (B), 2h (D), 12h (F), 24h (H), 36h (J), 48h (L), 60h (M) and 72h (N). Cultures in C-E and D-F were infected at an MOI of 100 to increase the likelihood of visualizing organisms in thin sections. Cultures in G-K and H-N were infected at an MOI of 10. Cultures in G-N were infected at an MOI of 10. Bar, 500 nm

E

	37°C	**33°C**
Uninfected	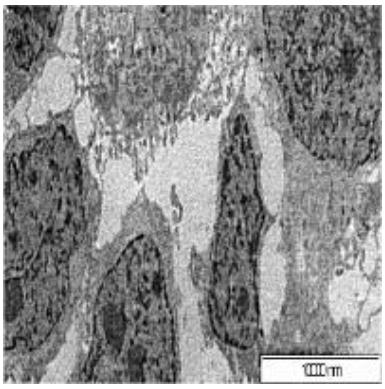	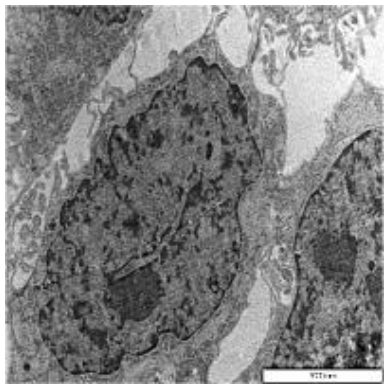
	A	**B**
2h	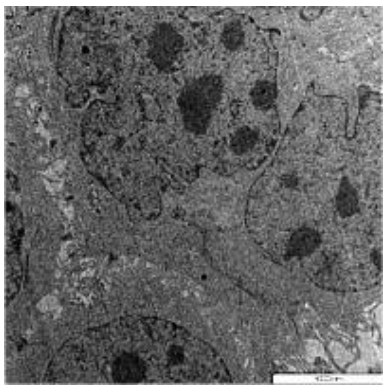	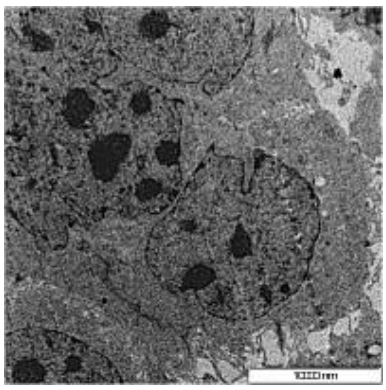
	C	**D**
12h	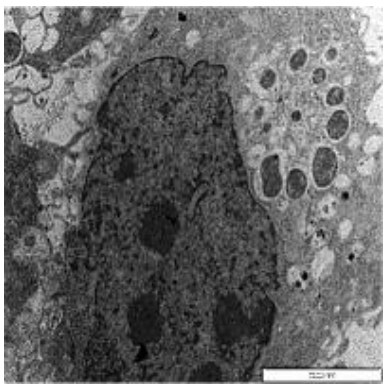	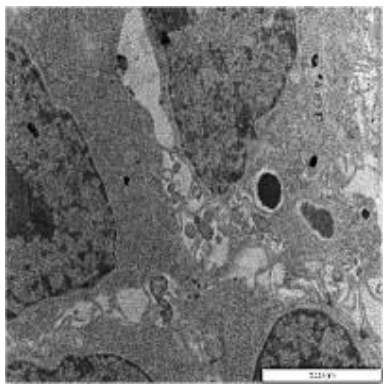
	E	**F**
24h	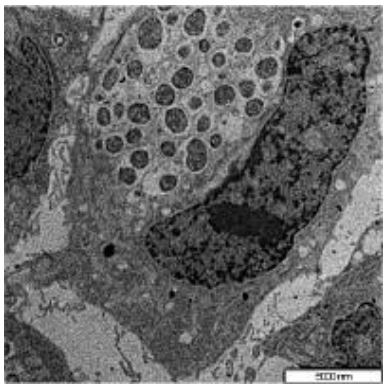	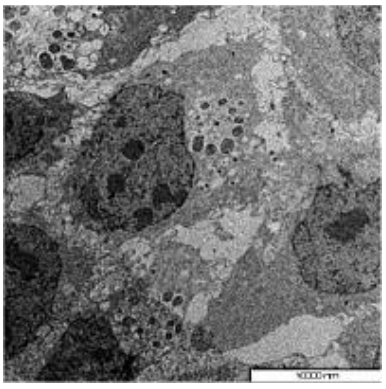
	G	**H**

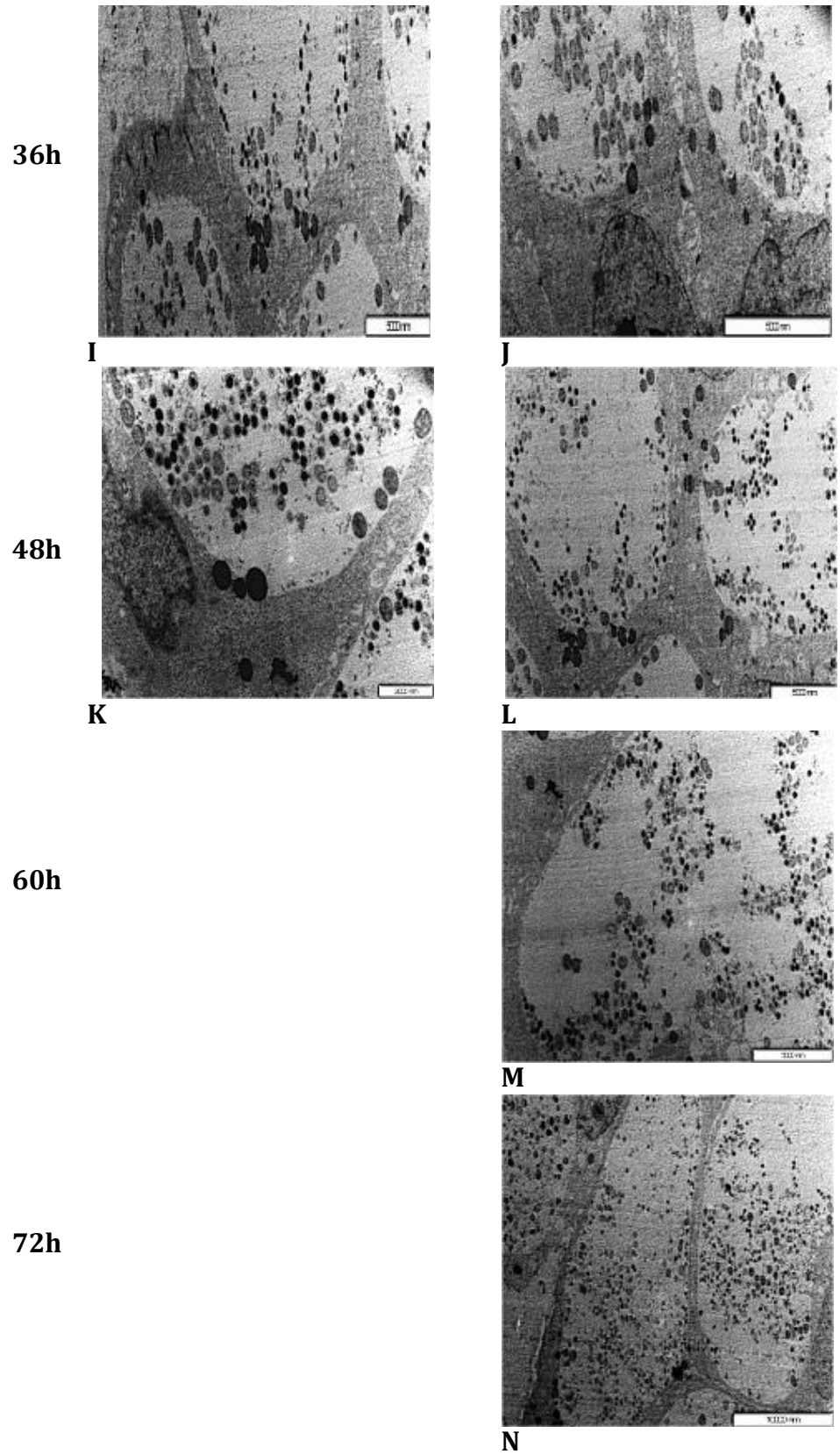

Figure 7: TEM micrographs of HaCaT cells infected with *C. trachomatis* US151 demonstrating differentiation, growth, division and redifferentiation at 37°C and 33°C over the course of the developmental

cycle. Uninfected (A), 2h (C), 12h (E), 24h (G), 36h (I) and 48h (K) post infection at 37^{o}C. Uninfected (B), 2h (D), 12h (F), 24h (H), 36h (J), 48h (L), 60h (M) and 72h (N). Cultures in C-E and D-F were infected at an MOI of 100 to increase the likelihood of visualizing organisms in thin sections. Cultures in G-K and H-N were infected at an MOI of 10. Cultures in G-N were infected at an MOI of 10. Bar, 500 nm.

CHAPTER 5: DISCUSSION

This study contributes to understanding the difference pathogenicity of the LGV biovar of *C. trachomatis* and its G (enital) biovar. LGV infection begins in the skin and the temperature of the skin is ± 33ºC. As the infection progresses to the secondary stage in the lymph nodes the temperature to which the chlamydia are exposed changes to the body core temperature which is 37ºC. Most research on the behaviour of chlamydia in cell culture, irrespective of the biovar, has been done at 37ºC. In addition, this research has been carried out in cell lines that are not its primary target cell and with reference strains of *C. trachomatis* whose behaviour may have been transformed by many years of *in vitro* propagation (Joubert and Sturm, 2011). Shaw et al. (2000), Belland et al. (2003) and Nicholson et al. (2003) performed genomic transcriptional analysis during the chlamydial developmental cycle. However, they restricted their analysis to one serovar, and thus, no information is available on comparative gene expression between serovars. Joubert and Sturm (2011) developed a model in which *C. trachomatis* is grown in human keratinocytes at 37 and 33 °C. They used fresh clinical isolates and the three ATCC LGV reference strains L1, L2 and L3. They concluded that this model more closely represents the conditions present at the primary infection site in LGV than other models published in the literature. These recommendations were applied in this study.

As Joubert and Sturm (2011), we used the HaCaT cell line, which is an immortalized human keratinocyte cell line that has a similar differentiation pattern to that of a normal keratinocyte (Boukamp, Breitkreutz et al. 1994). We also used clinical LGV isolate (L2 US151) in addition to an ATCC reference strain (L2 434). A clinical isolate of the Genital biovar (strain E) was used for comparison purposes. In addition, we used TEM

to correlate the transcriptional events and to confirm the stage of the organism in the developmental cycle at 37^{o}C and 33^{o}C

The chlamydial developmental cycle has been well characterized microscopically. However, the signals that stimulate conversion from EB to RB and vice versa are so far unknown. In addition, the mechanisms associated with the regulation of intracellular development are poorly understood (Wickstrum, Sammons et al. 2013). It has been shown that the synthesis of numerous proteins occurs throughout the chlamydial developmental cycle, while other proteins are associated with mid- and late-stage differentiation (Shaw, Dooley et al. 2000). This pattern of protein synthesis is consistent with the structural and functional characteristics of the chlamydial developmental cycle (Rosario and Tan 2016).

The previous identification of temporally regulated genes implicates an ordered system of developmental regulation and suggests that the developmental cycle is ultimately regulated at the transcriptional level (Shaw, Dooley et al. 2000, Belland, Zhong et al. 2003, Nicholson, Olinger et al. 2003). Early-, mid- and late-cycle genes represent a subset of genes that are important in understanding key events in the differentiation processes that control the developmental cycle (Belland, Zhong et al. 2003).

In this study we aimed to investigate the effect of temperature on chlamydial temporal gene expression in human keratinocytes.

Two early-cycle genes were quantified by RT-PCR. These are the inclusion protein gene *incB* and the chaperonin gene *groEL-1*. The findings confirmed these as early-cycle genes as they were expressed at every time point of the developmental cycle from

2 hours post infection, thus supporting previous reports using different experimental procedures. The family of inclusion proteins expressed during the chlamydial developmental cycle play an important role in modifying the inclusion membrane to support chlamydial intracellular survival and growth (Belland, Zhong et al. 2003). Modification and extension of this membrane takes place throughout the cycle but will decrease in the late stage.

At 37^{o}C, L2 434 showed an over 30-fold increase in *incB* expression level at 2 hours post infection, compared to L2 US151 in which a constantly lower level of expression was observed. IncB is one of a set of Inc proteins and we propose that our clinical LGV isolate uses one or more Inc proteins other than IncB. This difference may be on the account of the modification of strain LGV 434 during numerous passages in cell culture. The immediate increase in level of *incB* expression at 2 hours post infection by LGV 434 was not seen at 33^{o}C which indicates that modification of the nascent inclusions occurs at a faster rate at 37^{o}C than at 33^{o}C. This was in keeping with the chlamydial growth rate observed using the TEM. Furthermore, at 33^{o}C both L2 434 and US151 showed a fairly constant level of *incB* expression throughout the developmental cycle. This finding is due, in part, to the fact that LGV reference strains have been proved to grow significantly faster at 37^{o}C than 33^{o}C in HaCaT cells(Joubert and Sturm 2011). At both temperatures, *incB* expression levels peaked at 12 hours post infection for strain E. The difference in the pattern of gene expression observed for strain E could be correlated with the fact that the primary target for G strains are epithelial cells of the genital tract, and in this study keratinocytes were used.

At 37^{o}C and 33^{o} C, *groEL-1* expression levels remained fairly constant between 2 and 36 hours post infection for all tested strains. However, strain E at 37^{o}C and L2 US151 at 33^{o}C showed increased *groEL-1* expression levels at 48 hours post infection. *GroEL-*

1 is known to increase during nutrient deprivation (Karunakaran, Noguchi et al. 2003), which could be the case late in the cycle and thus have resulted in these findings.

The *C. trachomatis* genome contains genes that code for enzymes of glycolysis and pentose phosphate pathway enzymes and the genes encoding these enzymes have been named the mid-cycle chlamydial genes (Shaw, Dooley et al. 2000, Gérard, Freise et al. 2002). In the mid-cycle a number of cellular processes take place including energy metabolism, DNA replication and repair, protein folding and type III secretion system (TTSS). Expression of *pyk-F* of the glycolysis pathway and *tal* of the pentose phosphate pathway were analyzed in this study as representatives of the mid-cycle genes.

The RT-PCR analysis indicates that the proteins required for energy metabolism are present throughout the chlamydial developmental cycle in keratinocytes at 37^{o}C and 33^{o}C. However, the two genes studied are expressed at different levels amongst the tested chlamydial strains. *Pyk-F* expression was most abundant at 2 hours post infection at 37^{o}C in all tested chlamydial strains, indicating that energy is required immediately following invasion of chlamydia into the keratinocytes. This differs from what is seen in HeLa cells with strain E where no expression of *pyk-F* was seen in the early phase (Table 4.2). *Tal* on the other hand was expressed the highest at 12 hours post infection for strain E, which correlates with rapid growth and division of RBs. This is consistent with the electron microscopic observations (Fig. 7E). At 33^{o}C, the metabolically active stage of the cycle was delayed, as both *pyk* and *tal* were most abundant from 24 hours post infection. This was also consistent with the TEM observations in which the metabolically active RB form was only observed from 24 hours post infection at 33^{o}C (Fig. 7H).

Two late-cycle genes that have been reported to be expressed from 24 hours post infection were also analyzed. These are *hctA* that encodes chlamydial histone-like protein and mediates chromosomal condensation during the differentiation of RBs to EBs, and *omcB* that encodes cysteine rich outer membrane protein that interact with the MOMP to form this complex which involves extensive protein cross linking through the formation of cysteine bonds (Belland, Zhong et al. 2003).

At 37^{o}C an increase in *hctA* expression was observed at 2 hours post infection and decreased by 1- fold at 12 hours post infection for L2 434 and serovar E. This could be due to the fact that at 2 hours post infection chlamydia still has highly condensed chromosome. This is supported by the high *hctA* expression in the early phase. Condensed chromatin of EB is dispersed as differentiation into pleomorphic RB occurs, and as this occurs the expression of *hctA* is downregulated (Tattersall, Rao et al. 2012). *hctA* expression levels remained fairly constant form 2 to 36 hours post infection for L2 US151. The fact that this was isolated from an ulcer in primary stage of infection might have affected the normal regulation of *ihtA* and *hctA* expression. Expression of *hctA* is tightly regulated and is repressed by the small non-coding RNA, IhtA until RB to EB redifferentiation (Grieshaber, Grieshaber et al. 2006). IhtA regulate the translation of a target mRNA during specific developmental stages. *IhtA* is transcribed early in the infection process to repress expression of *hctA*. Late in infection, *IhtA* transcription decreases allowing HctA synthesis to occur and RB to EB differentiation to proceed (Altuvia 2004, Grieshaber, Grieshaber et al. 2006). A different expression pattern was observed at 33^{o}C; *hctA* expression was abundant from 24 hours post infection for L2 434 and US151, although *hctA* was still expressed in low levels at 2 and 12 hours post infection. Strain E had two expression peaks of *hctA,* at 24 and 72

hours post infection. This suggests that by 72 hours post infection strain E was 24 hours in a second cycle. Previous studies reported that *hctA* is not expressed until 24 hours post infection in HeLa cells. However, our study shows that in keratinocytes *hctA* is expressed throughout the chlamydial developmental cycle but the level of expression increases from 24 hours post infection.

Like *hctA*, at 37ºC strain L2 434 showed high *omcB* expression level at 2 hours post infection. At 12 hours post infection the expression level was suppressed, but upregulated again at 24 hours post infection. These findings suggest that chlamydia is still in a EB form at 2 hours post infection in keratinocytes, as *omcB* is only found in EBs as the component of the disulphide-linked outer membrane protein complex that confers structural stability to EBs (Shaw, Dooley et al. 2000). L2 US151 however showed a different expression pattern compared to L2 434. *OmcB* expression level remained fairly constantly low throughout the chlamydial developmental cycle. This was the case for *hctA* expression as well. This could mean that the clinical L2 isolates circulating have a different regulatory system for gene expression as the laboratory L2 strain. Another possibility is the fact that the two L2 isolates studied were isolated at different sites of infection could have affected the gene expression regulatory system. Lastly, in our population LGV presents in the primary stage as a painful genital ulcer without the tendency to resolve spontaneously. This could mean that there is a genetic difference between LGV strains that is responsible for this difference in clinical presentation (Sturm, Moodley et al. 2005). Strain E also showed a different pattern of *omcB* expression; fairly low expression levels were observed in the late-cycle compared to early- and mid-cycle. These findings suggest that chlamydial gene expression differs amongst the target cells for different chlamydial biovars.

At 33ºC, Both L2 reference strains and strain E only expressed *omcB* from 24 hours post infection and increased at 36 hours post infection. This was consistent with the TEM, which showed numerous EBs at 36 hours post infection. These findings are the same as previously published reports in HeLa cells at 37ºC. At 60 and 72 hours post infection *omcB* expression was suppressed in L2 434 and US151, indicating that the L2 chlamydial life cycle is completed by 48 hours post infection in keratinocytes at 33ºC. Furthermore, strain E showed some expression of the late cycle genes at 60 and 72 hours post infection, indicating that the developmental cycle for strain E can go on up to 72 hours. This was also consistent with the TEM, which showed numerous EBs that were still compartmentalized within the inclusion at 60 and 72 hours post infection.

CHAPTER 6: CONCLUSIONS

Mid- and late-cycle chlamydial gene expression levels in keratinocytes are different to the published research conducted in HeLa cells. The mid- and late-cycle genes were expressed throughout the chlamydial developmental cycle in keratinocytes. These observations were reproducible. Furthermore, the reliability of the methods applied was confirmed by performing the same experiments in HeLa cells and in our hands results in HeLa cells were as published.

C. trachomatis metabolism rate is less at 33^{o}C than at 37^{o}C. This was indicated by decreased *pyk-F* and *tal* expression levels at 33^{o}C. This was also confirmed by TEM in which the metabolically active RB form and redifferentiation to EBs was delayed at 33^{o}C. This supports the observation in this and a previous study (Joubert and Sturm 2011) that *C. trachomatis* replicates faster at 37^{o}C than at 33^{o}C.

This study confirms that temperature has an effect on the level of chlamydial gene expression when grown in keratinocytes. This is important for further studies on the pathogenesis of LGV.

At 2 hours post infection chlamydia still retains its EB structural conformation in keratinocytes at 37^{o}C. This was indicated by high expression levels of late-cycle genes at 2 hours post infection at 37^{o}C.

The L2 reference strain 434 is different than the clinical L2 US151as indicated by the difference in the gene expression pattern. There are several explanations for this. The reference strain could have undergone genetic changes during numerous passages *in*

vitro, gene expression patterns could differ between isolates from ulcers (L2 US151) and those from lymphnode aspirates (L2 434) or current LGV strains could differ from historical strains since the clinical presentation differs from the textbook description. This last difference could be restricted to strains circulating in the KZN population or be more general.

CHAPTER 7 – REFERENCES

Altuvia, Shoshy. (2004). Regulatory small RNAs: the key to coordinating global regulatory circuits. *J Bacteriol, 186*(20), 6679-6680.

Beagley, Kenneth W, & Timms, Peter. (2000). *Chlamydia trachomatis* infection: incidence, health costs and prospects for vaccine development. *Journal of reproductive immunology, 48*(1), 47-68.

Beatty, Wandy L, Morrison, Richard P, & Byrne, Gerald I. (1994). Persistent chlamydiae: from cell culture to a paradigm for chlamydial pathogenesis. *Microbiological reviews, 58*(4), 686-699.

Bébéar, C, & De Barbeyrac, B. (2009). Genital *Chlamydia trachomatis* infections. *Clinical Microbiology and Infection, 15*(1), 4-10.

Belland, R. J., Zhong, G., Crane, D. D., Hogan, D., Sturdevant, D., Sharma, J., . . . Caldwell, H. D. (2003). Genomic transcriptional profiling of the developmental cycle of Chlamydia trachomatis. *Proc Natl Acad Sci U S A, 100*(14), 8478-8483. doi: 10.1073/pnas.1331135100

Black, Carolyn M. (1997). Current methods of laboratory diagnosis of Chlamydia trachomatis infections. *Clinical Microbiology Reviews, 10*(1), 160-184.

Biosystems, A. (2004). "Guide to performing relative quantitation of gene expression using real-time quantitative PCR." Applied Biosystems, Foster City: 28-30.

Boukamp, P, Breitkreutz, D, Hulsen, A, Tomakidi, P, & Fusenig, NE. (1994). In vitro transformation and tumor progression: a multistep model for skin carcinogenesis. *The Keratinocyte Handbook (M. Leigh, B. Lane and FM Watt, Eds.)*, 485-499.

Caldwell, HD, Kromhout, J, & Schachter, J. (1981). Purification and partial characterization of the major outer membrane protein of Chlamydia trachomatis. *Infect Immun, 31*(3), 1161-1176.

Carlson, J. H., Porcella, S. F., McClarty, G., & Caldwell, H. D. (2005). Comparative genomic analysis of *Chlamydia trachomatis* oculotropic and genitotropic strains. *Infect Immun, 73*(10), 6407-6418. doi: 10.1128/IAI.73.10.6407-6418.2005

Darville, Toni, & Hiltke, Thomas J. (2010). Pathogenesis of genital tract disease due to Chlamydia trachomatis. *Journal of Infectious Diseases, 201*(Supplement 2), S114-S125.

Debattista, Joseph, Timms, Peter, Allan, John, & Allan, Janet. (2003). Immunopathogenesis of *chlamydia trachomatis* infections in women. *Fertility and sterility, 79*(6), 1273-1287.

Feher, Victoria A, Randall, Arlo, Baldi, Pierre, Bush, Robin M, Luis, M, & Amaro, Rommie E. (2013). A 3-dimensional trimeric β-barrel model for Chlamydia MOMP contains conserved and novel elements of Gram-negative bacterial porins. *PloS one*, *8*(7), e68934.

Fields, KA, Fischer, E, & Hackstadt, T. (2002). Inhibition of fusion of *Chlamydia trachomatis* inclusions at 32 C correlates with restricted export of IncA. *Infect Immun*, *70*(7), 3816-3823.

Fothergill-Gillmore, LA, Rigden, DJ, Michels, PA, & Phillips, SE. (2000). Leishmania pyruvate kinase: the crystal structure reveals the structural basis of its unique regulatory properties. *Biochemical Society Transactions*, *28*(2), 186-190.

Fothergill-Gilmore, Linda A, & Michels, Paul AM. (1993). Evolution of glycolysis. *Progress in biophysics and molecular biology*, *59*(2), 105-235.

Frohlich, K, Hua, Ziyu, Quayle, Alison J, Wang, Jin, Lewis, Maria E, Chou, Chau-wen, . . . Shen, Li. (2014). Membrane vesicle production by Chlamydia trachomatis as an adaptive response. *Front Cell Infect Microbiol*, *4*.

Gérard, Hervé C, Freise, Julia, Wang, Zhao, Roberts, George, Rudy, Debbi, Krauß-Opatz, Birgit, . . . Whittum-Hudson, Judith A. (2002). *Chlamydia trachomatis* genes whose products are related to energy metabolism are expressed

differentially in active vs. persistent infection. *Microbes and infection*, *4*(1), 13-22.

Grieshaber, Nicole A, Grieshaber, Scott S, Fischer, Elizabeth R, & Hackstadt, Ted. (2006). A small RNA inhibits translation of the histone- like protein Hc1 in Chlamydia trachomatis. *Molecular microbiology*, *59*(2), 541-550.

Hammerschlag, M. R. (2002). The intracellular life of chlamydiae. *Semin Pediatr Infect Dis*, *13*(4), 239-248. doi: 10.1053/spid.2002.127201

Hanada, Hirofumi, Ikeda-Dantsuji, Yurika, Naito, Masatoshi, & Nagayama, Ariaki. (2003). Infection of human fibroblast-like synovial cells with *Chlamydia trachomatis* results in persistent infection and interleukin-6 production. *Microbial pathogenesis*, *34*(2), 57-63.

Hou, S., Lei, L., Yang, Z., Qi, M., Liu, Q., & Zhong, G. (2013). *Chlamydia trachomatis* outer membrane complex protein B (OmcB) is processed by the protease CPAF. *J Bacteriol*, *195*(5), 951-957. doi: 10.1128/JB.02087-12

Iliffe- Lee, Emma R, & McClarty, Grant. (1999). Glucose metabolism in *Chlamydia trachomatis*: the ‘energy parasite’hypothesis revisited. *Molecular microbiology*, *33*(1), 177-187.

Iliffe- Lee, Emma R, & McClarty, Grant. (2002). Pyruvate kinase from *Chlamydia trachomatis* is activated by fructose- 2, 6- bisphosphate. *Molecular microbiology, 44*(3), 819-828.

Joubert, Bronwyn C. (2010). *The interaction of lymphogranuloma venereum and oculogenital chlamydia trachomatis with human keratinocytes and cervical epithelium.*

Joubert, B. C. and A. W. Sturm (2011). "Differences in *Chlamydia trachomatis* growth rates in human keratinocytes among lymphogranuloma venereum reference strains and clinical isolates." J Med Microbiol 60(Pt 11): 1565-1569.

Karunakaran, Karuna P, Noguchi, Yasuyuki, Read, Timothy D, Cherkasov, Artem, Kwee, Jeffrey, Shen, Caixia, . . . Brunham, Robert C. (2003). Molecular analysis of the multiple GroEL proteins of Chlamydiae. *J Bacteriol, 185*(6), 1958-1966.

Liechti, GW, Kuru, E, Hall, E, Kalinda, A, Brun, YV, VanNieuwenhze, M, & Maurelli, AT. (2014). A new metabolic cell-wall labelling method reveals peptidoglycan in Chlamydia trachomatis. *Nature, 506*(7489), 507-510.

Mathews, S, George, Carmel, Flegg, Cameron, Stenzel, D, & Timms, Peter. (2001). Differential expression of ompA, ompB, pyk, nlpD and Cpn0585 genes between normal and interferon-γ treated cultures of *Chlamydia pneumoniae*. *Microbial pathogenesis, 30*(6), 337-345.

Mayer, J, Woods, ML, Vavrin, Z, & Hibbs, JB. (1993). Gamma interferon-induced nitric oxide production reduces *Chlamydia trachomatis* infectivity in McCoy cells. *Infect Immun, 61*(2), 491-497.

Mital, Jeffrey, Miller, Natalie J, Dorward, David W, Dooley, Cheryl A, & Hackstadt, Ted. (2013). Role for chlamydial inclusion membrane proteins in inclusion membrane structure and biogenesis. *PloS one, 8*(5), e63426.

Moulder, JAMES W. (1991). Interaction of chlamydiae and host cells in vitro. *Microbiological reviews, 55*(1), 143.

Mukhopadhyay, Sanghamitra, Good, David, Miller, Richard D, Graham, James E, Mathews, Sarah A, Timms, Peter, & Summersgill, James T. (2006). Identification of Chlamydia pneumoniae proteins in the transition from reticulate to elementary body formation. *Molecular & Cellular Proteomics, 5*(12), 2311-2318.

Newhall, WJ t. (1987). Biosynthesis and disulfide cross-linking of outer membrane components during the growth cycle of Chlamydia trachomatis. *Infect Immun, 55*(1), 162-168.

Nicholson, Tracy L, Olinger, Lynn, Chong, Kimberley, Schoolnik, Gary, & Stephens, Richard S. (2003). Global stage-specific gene regulation during the

developmental cycle of Chlamydia trachomatis. *J Bacteriol, 185*(10), 3179-3189.

Niehus, E., Cheng, E., & Tan, M. (2008). DNA supercoiling-dependent gene regulation in Chlamydia. *J Bacteriol, 190*(19), 6419-6427. doi: 10.1128/JB.00431-08

Omsland, Anders, Sager, Janet, Nair, Vinod, Sturdevant, Daniel E, & Hackstadt, Ted. (2012). Developmental stage-specific metabolic and transcriptional activity of Chlamydia trachomatis in an axenic medium. *Proceedings of the National Academy of Sciences, 109*(48), 19781-19785.

Omsland, Anders, Sixt, Barbara Susanne, Horn, Matthias, & Hackstadt, Ted. (2014). Chlamydial metabolism revisited: interspecies metabolic variability and developmental stage-specific physiologic activities. *FEMS Microbiol Rev, 38*(4), 779-801.

Pannekoek, Y., van der Ende, A., Eijk, P. P., van Marle, J., de Witte, M. A., Ossewaarde, J. M., . . . Dankert, J. (2001). Normal IncA expression and fusogenicity of inclusions in *Chlamydia trachomatis* isolates with the incA I47T mutation. *Infect Immun, 69*(7), 4654-4656. doi: 10.1128/IAI.69.7.4654-4656.2001

Phillips-Campbell, R, Kintner, J, & Schoborg, RV. (2014). Induction of the Chlamydia muridarum stress/persistence response increases azithromycin

treatment failure in a murine model of infection. *Antimicrobial agents and chemotherapy, 58*(3), 1782-1784.

Pilhofer, Martin, Aistleitner, Karin, Biboy, Jacob, Gray, Joe, Kuru, Erkin, Hall, Edward, . . . Horn, Matthias. (2013). Discovery of chlamydial peptidoglycan reveals bacteria with murein sacculi but without FtsZ. *Nature communications, 4*.

Rosario, Christopher J, & Tan, Ming. (2016). Regulation of Chlamydia Gene Expression by Tandem Promoters with Different Temporal Patterns. *J Bacteriol, 198*(2), 363-369.

Sardinia, Lisa M, Segal, Ellyn, & Ganem, Don. (1988). Developmental regulation of the cysteine-rich outer-membrane proteins of murine Chlamydia trachomatis. *Journal of general microbiology, 134*(4), 997-1004.

Schachter, J, & Osoba, AO. (1983). Lymphogranuloma venereum. *British Medical Bulletin, 39*(2), 151-154.

Schachter, Julius. (1999). Infection and disease epidemiology. *Chlamydia: intracellular biology, pathogenesis, and immunity. ASM Press, Washington, DC*, 139-169.

Schramm, Nara, & Wyrick, Priscilla B. (1995). Cytoskeletal requirements in Chlamydia trachomatis infection of host cells. *Infect Immun, 63*(1), 324-332.

Shaw, EI, Dooley, CA, Fischer, ER, Scidmore, MA, Fields, KA, & Hackstadt, T. (2000). Three temporal classes of gene expression during the Chlamydia trachomatis developmental cycle. *Molecular microbiology, 37*(4), 913-925.

Sherrid, A. M. and K. Hybiske (2017). "Chlamydia trachomatis cellular exit alters interactions with host dendritic cells." Infection and Immunity **85**(5): e00046-00017.

Siegl, A, Horn, M, Tan, M, & Bavoil, P. (2012). Lessons from environmental chlamydiae. *Intracellular Pathogens I: Chlamydiales*, 51-73.

Söderlund, G, & Kihlström, E. (1982). Physicochemical surface properties of elementary bodies from different serotypes of chlamydia trachomatis and their interaction with mouse fibroblasts. *Infect Immun, 36*(3), 893-899.

Stephens, Richard S, Kalman, Sue, Lammel, Claudia, Fan, Jun, Marathe, Rekha, Aravind, L, . . . Zhao, Qixun. (1998). Genome sequence of an obligate intracellular pathogen of humans: Chlamydia trachomatis. *Science, 282*(5389), 754-759.

Sturm, P. D., et al. (2005). "Molecular diagnosis of lymphogranuloma venereum in patients with genital ulcer disease." Journal of clinical microbiology 43(6): 2973-2975.

Tattersall, J., Rao, G. V., Runac, J., Hackstadt, T., Grieshaber, S. S., & Grieshaber, N. A. (2012). Translation inhibition of the developmental cycle protein HctA by the small RNA IhtA is conserved across Chlamydia. *PloS one, 7*(10), e47439. doi: 10.1371/journal.pone.0047439

Todd, William J, & Caldwell, Harlan D. (1985). The interaction of Chlamydia trachomatis with host cells: ultrastructural studies of the mechanism of release of a biovar II strain from HeLa 229 cells. *Journal of Infectious Diseases, 151*(6), 1037-1044.

Wang, Yan, Berg, Eric A, Feng, Xiaogeng, Shen, Li, Smith, Temple, Costello, Catherine E, & Zhang, You- Xun. (2006). Identification of surface- exposed components of MOMP of Chlamydia trachomatis serovar F. *Protein science, 15*(1), 122-134.

Ward, ME. (1983). Chlamydial classification, development and structure. *British Medical Bulletin, 39*(2), 109-115.

Wickstrum, Jason, Sammons, Lindsay R, Restivo, Keasha N, & Hefty, P Scott. (2013). Conditional gene expression in *Chlamydia trachomatis* using the tet system. *PloS one, 8*(10), e76743.

Wyrick, P. B. (2010). *Chlamydia trachomatis* persistence in vitro: an overview. *J Infect Dis, 201 Suppl 2*, S88-95. doi: 10.1086/652394

Young, Richard A, & Elliott, Timothy J. (1989). Stress proteins, infection, and immune surveillance. *Cell, 59*(1), 5-

APPENDIX A – REAGENTS AND MEDIA

Phosphate buffered saline (PBS) (Dulbecco A)

5 PBS tablets (Oxoid)

500ml-distilled water

Five PBS tablets were dissolved in 500ml autoclaved distilled water. The PBS was autoclaved at 121^{o}C for 10 minutes, then decanted into 20ml aliquots and refrigerated until use.

0.05% EDTA

0.05g EDTA

1 PBS tablet

100ml-distilled water

One PBS tablet and 0.05g EDTA were dissolved in approximately in 80ml autoclaved distilled water. The pH was adjusted to approximately 7.4 using 7.5% sodium bicarbonate and the volume brought up to 100ml. The solution was autoclaved at 121^{o}C for 10 minutes, pipetted into 1ml aliquots and refrigerated until use.

GTC

5 M guanidinum thiocyanate (60 g/100 ml)

0.5% sodium-*N*-lauryl sarcosine (0.5 g/100 ml)

25 mM tri-sodium citrate (1 g/100 ml)

0.1 M 2-mercaptoethanol (BME) (0.7 ml/100 ml)

60 g of 5 M GTC, 0.5 g of 0.5% sodium-*N*-lauryl sarcosine and 1 g of 25 mM tri-sodium citrate were dissolved in 100 ml autoclaved distilled water. The solution was left over night to dissolve. On the day of use, 0.7 ml of 0.1 M 2-mercaptoethanol was added to the solution.

2 % agarose gel

4 g agarose

200 ml 1x TAE buffer

4 g of agarose was dissolved in 200 ml 1 x TAE buffer swirling and heating in the microwave. The mixture was allowed to cool then poured into the casting tray.

HaCaT cell freezing fluid

30ml RPMI-1640 with L-glutamine and HEPES

10ml glycerol

10ml FBS

Ten milliliters of glycerol and 10ml of FBS were added to 30ml of RPMI-1640 and the solution filter-sterilized into a sterile container.

Sucrose-Phosphate-Glutamate Buffer (SPG)

Sucrose

KH_2PO_4

$Na_2HPO_4.7H_2O$

Glutamic acid

Distilled water

The sucrose, KH_2PO_4, $Na_2HPO_4.7H_2O$ and glutamic acid were dissolved in approximately in 400ml autoclaved distilled water, the pH was adjusted to approximately 7.4 using 7.5% sodium bicarbonate and the volume brought up to 500ml. The solution was filter sterilized through a 0.22Lm filter, then aliquoted and stored at -20 ^oC until use.

2% Glutaraldehyde Solution

4 ml 25% glutaraldehyde

48ml EMEM

Glutaraldehyde was added to EMEM and mixed thoroughly

Spurr resin

4.1 g 4221-3, 4-Epoxycyclohexanemythyl 3, 4-epoxycyclohexaminecarboxylate (ERL)

5.9 g Nonenyl succinic anhydride (NSA)

1.43 g 736-Didlycidyl ether (DER)

0.1 g Dimethylaminoethanol (DMAE)

ERL, NSA and DER were added together and allowed to mix for 15 minutes. Thereafter, DMAE was also added and allowed to mix for a further 15 minutes

Lead citrate

1.33 g lead nitrate

1.76 g sodium citrate

8 ml NaOH

50 ml distilled water

Lead nitrate and sodium citrate were added to 30 ml distilled water in a 50 ml capacity stopped flask. The solution was mixed by shaking for 1 minute. The solution was then allowed to stand for 30 minutes, shaking at intervals. 8 ml of NaOH was also added and the solution was made up to 50 ml with distilled water. The solution was allowed to stand until clear before use.

Uranyl citrate

2 % uranyl citrate was prepared by dissolving 2 g of uranyl citrate powder in 100 ml distilled water. It was centrifuged for 15 minutes and refrigerated until required.

APPENDIX B – CALCULATIONS

1. Validation experiment calculations

For a valid $\Delta\Delta C_T$ calculation, the efficiency of the target amplification must be approximately equal. This is determined by looking at how ΔC_T varies with template dilution

$$\Delta C_T = C_{T\,(target)} - C_{T\,(reference)}$$

E.g. Table 1: ΔC_T calculations for the validation experiment

Input mount cDNA (ng)	Log of input amount: ng cDNA	*groEL-1* average C_T	*16SrRNA* average C_T	ΔC_T *groEL-1 – 16SrRNA*
100	2	26.76	23.77	2.99
10	1	30.45	27.56	2.88
1	0	33.45	30.15	2.97
0.1	-1	33.12	33.62	2.81
0.01	-2	38.46	35.35	3.11

For a passing validation experiment, the absolute value of the slope should be < 0.1. The equation of the regression line is displayed on the graph. The slope of the line is "**m**" in the equation.

$$Y = \mathbf{m}x + b$$

2. The comparative C_T ($\Delta\Delta C_T$) calculations

   Step 1: The mean C_T and standard deviation values of the replicate sample were calculated.

Step 2: The ΔC_T values were calculated.

The ΔC_T values were calculated by:

$$\Delta C_T = C_{T\ target} - C_{T\ reference}$$

E.g. the average reference gene *16SrRNA* C_T value was subtracted from the C_T value of target gene *groEL-1* and yielded the value of -5.42

GroEL-1 $\Delta C_T = 29.73 - 35.15$
$= -5.42$

Step 3: The standard deviations for the ΔC_T values were calculated

- The standard deviation of the ΔC_T value was calculated from the standard deviations of the target and reference values using the formula:

$S = (S_1^{\,2} + S_2^{\,2})^{1/2}$; where $X^{1/2}$ is the square root of X and S = standard deviation

E.g. to calculate the standard deviation of *groEL-1* ΔC_T value:

$S_1 = 0.12$ and $S_2 = 0.21$
$S_1^{\,2} = 0.01$ and $S_2^{\,2} = 0.04$
$S = (0.01 + 0.04)^{½}$
$S = 0.23$

Therefore, *groEL-1* $\Delta C_T = (29.73 \pm 0.01) - (35.15 \pm 0.21)$
$= -5.42 \pm 0.23$

Step4: Calculate the $\Delta\Delta C_T$ value

The $\Delta\Delta C_T$ value was calculated by:

$$\Delta\Delta C_T = \Delta C_{T\ test\ sample} - \Delta C_{T\ calibrator\ sample}$$

For example, subtracting the ΔC_T calibrator *groEL-1* (from the validation experiment) from the ΔC_T of *groEL-1* (test sample) yields the value of 0.28

$\Delta\Delta C_T = 3.23 - 2.95 = 0.28$

Step5: Incorporating the standard deviation of $\Delta\Delta C_T$ values into the fold-difference.

- Fold-differences calculated using the $\Delta\Delta C_T$ are expressed as a range, which is the result of incorporating the standard deviation of the $\Delta\Delta C_T$ into the fold-difference calculation.
- The range for target is calculated by:

  $2^{-\Delta\Delta Ct}$ with $\Delta\Delta C_T + s$ and $\Delta\Delta C_T - s$, where s is the standard deviation of the $\Delta\Delta C_T$ value

  For example, *groEL-1* at 33^{o}C, 2h post infection had a 0.71 to 0.97 fold-difference in expression relative to the calibrator *groEL-1*.

  $\Delta\Delta C_T + s = 0.28 + 0.23 = 0.51$
  $2^{-\Delta\Delta Ct} = 2^{-(0.51)} = 0.71$

  And

  $\Delta\Delta C_T - s = 0.28 - 0.23 = 0.05$
  $2^{-\Delta\Delta Ct} = 2^{-(0.05)} = 0.97$

  Mean = 0.84

APPENDIX C – RAW DATA

1. HaCaT 37°C C_T and standard deviation values

	***16SrRNA* CT values**														
	L2					**E**					**US151**				
	2h	**12h**	**24h**	**36h**	**48h**	**2h**	**12h**	**24h**	**36h**	**48h**	**2h**	**12h**	**24h**	**36h**	**48h**
run1	41,21	42,24	23,96	22,99	34,32	35,92	34,89	21,73	19,35	33,85	34,89	38,98	23,99	23,53	33,69
run1	41,22	41,10	23,99	23,35	35,37	35,07	34,77	21,62	18,97	34,25	34,92	39,26	24,06	23,52	33,89
run1	42,17	41,01	24,33	23,24	35,60	36,08	34,70	21,78	18,78	33,89	35,16	38,02	23,92	23,32	33,72
run2	45,17	42,86	23,09	24,61	28,55	37,07	38,19	24,15	19,97	36,12	45,64	40,95	26,82	26,63	33,43
run2	41,29	40,44	22,66	24,56	28,25	37,47	37,78	23,95	20,02	36,36	Undetermined	41,55	26,77	26,87	33,17
run2	42,06	42,86	22,95	24,56	28,41	37,45	37,17	24,05	19,57	36,46	Undetermined	41,55	26,61	26,95	32,83
run3	Undetermined	40,95	25,65	26,47	33,51	39,17	36,30	28,01	26,99	36,13	45,97	41,73	27,54	26,91	35,19
run3	45,02	40,32	25,36	26,67	33,68	38,98	35,97	27,89	26,78	36,43	Undetermined	43,59	27,74	27,40	35,57

run3	44,25	40,36	25,42	26,65	33,67	38,49	36,30	26,90	27,06	36,23	Undetermined	41,91	27,24	27,14	35,45

	***16SrRNA* standard deviation**														
	L2					**E**					**US151**				
	2h	**12h**	**24h**	**36h**	**48h**	**2h**	**12h**	**24h**	**36h**	**48h**	**2h**	**12h**	**24h**	**36h**	**48h**
run1	0,55	0,69	0,21	0,18	0,69	0,54	0,10	0,09	0,14	0,22	0,15	0,65	0,07	0,12	0,11
run2	2,05	1,40	0,03	0,22	0,15	0,22	0,52	0,10	0,35	0,18		0,35	0,11	0,17	0,30
run3	0,55	0,35	0,15	0,11	0,09	0,35	0,19	0,61	0,15	0,15		1,03	0,26	0,24	0,19

	***IncB* CT values**														
	L2					E					US151				
	2h	12h	24h	36h	48h	2h	12h	24h	36h	48h	2h	12h	24h	36h	48h
run1	Undetermined	Undetermined	31,98	31,49	40,01	38,65	38,08	28,96	31,46	39,60	41,25	41,34	28,97	37,60	31,74
run1	Undetermined	Undetermined	31,85	31,34	40,42	38,98	37,58	29,13	31,68	40,85	42,20	41,54	28,34	37,91	31,85
run1	Undetermined	Undetermined	31,63	30,91	41,27	39,11	38,25	29,11	31,58	40,33	42,45	40,83	29,21	37,93	31,97
run2	37,20	Undetermined	32,58	32,34	32,10	37,60	39,53	26,18	30,14	38,35	34,77	37,01	26,97	26,79	28,06
run2	38,07	Undetermined	31,97	32,28	31,65	37,68	40,40	26,25	29,89	38,48	34,73	36,90	26,96	26,59	27,99

run2	38,37	Undetermined	32,42	32,00	31,67	37,19	39,96	26,05	29,86	38,79	34,96	37,05	27,01	26,59	28,06
run3	Undetermined	Undetermined	31,99	22,18	40,02	35,92	34,97	32,39	28,16	35,35	38,97	36,96	27,19	27,48	34,55
run3	Undetermined	Undetermined	31,71	22,18	39,96	35,81	34,94	32,82	28,50	35,31	39,21	36,40	27,17	27,86	34,14
run3	Undetermined	Undetermined	31,82	21,72	39,04	35,95	34,57	32,77	28,59	35,38	39,23	36,43	27,11	27,86	34,42

	***IncB* standard deviation**														
	L2					E					US151				
	2h	12h	24h	36h	48h	2h	12h	24h	36h	48h	2h	12h	24h	36h	48h
run1			0,35	0,35	0,35	0,23	0,35	0,09	0,11	0,63	0,63	0,37	0,45	0,18	0,11
run2	0,61		0,32	0,18	0,26	0,26	0,43	0,10	0,15	0,22	0,12	0,08	0,03	0,12	0,04
run3			0,14	0,34	0,54	0,07	0,22	0,24	0,23	0,04	0,15	0,32	0,04	0,19	0,21

	***Pyk-F* CT values**														
	L2					**E**					**US151**				
	2h	**12h**	**24h**	**36h**	**48h**	**2h**	**12h**	**24h**	**36h**	**48h**	**2h**	**12h**	**24h**	**36h**	**48h**
run1	37,56	37,41	24,92	23,96	34,58	33,58	33,92	22,68	29,05	33,10	35,92	37,10	25,52	24,90	34,13

run1	38,40	37,98	25,05	23,96	33,51	33,69	33,73	22,83	28,85	33,04	35,56	36,31	25,61	24,86	34,30
run1	37,82	37,49	25,14	23,86	35,27	34,10	33,83	22,78	29,08	33,07	35,49	36,77	25,59	24,88	34,37
run2	38,44	38,70	24,93	23,82	33,96	34,95	35,94	24,66	28,00	35,05	38,58	39,73	27,55	26,82	36,24
run2	37,93	38,61	24,78	23,75	34,03	35,42	36,18	24,53	28,10	35,46	38,01	39,74	27,65	26,93	36,51
run2	37,81	38,20	24,91	23,66	34,34	35,64	36,34	24,69	27,91	35,72	38,14	38,40	27,65	26,76	37,24
run3	42,98	40,08	25,48	25,91	36,31	35,99	36,35	27,62	27,23	35,50	37,98	39,72	27,26	26,73	36,13
run3	39,53	38,93	25,47	25,87	36,74	35,97	36,94	28,27	27,28	35,19	38,41	39,82	27,19	26,62	35,89
run3	39,36	38,78	25,48	25,93	36,43	35,41	37,26	27,63	27,05	35,39	38,94	38,65	27,23	26,61	36,47

	***Pyk-F* standard deviation**														
	L2					**E**					**US151**				
	2h	**12h**	**24h**	**36h**	**48h**	**2h**	**12h**	**24h**	**36h**	**48h**	**2h**	**12h**	**24h**	**36h**	**48h**
run1	0,43	0,69	0,11	0,06	0,89	0,27	0,10	0,08	0,05	0,03	0,23	0,40	0,05	0,02	0,13
run2	0,33	0,27	0,08	0,08	0,21	0,35	0,20	0,09	0,06	0,34	0,30	0,77	0,06	0,09	0,52
run3	2,04	0,71	0,01	0,03	0,22	0,33	0,46	0,38	0,12	0,16	0,48	0,65	0,03	0,07	0,30

***Tal* CT values**														
L2					**E**					**US151**				
2h	**12h**	**24h**	**36h**	**48h**	**2h**	**12h**	**24h**	**36h**	**48h**	**2h**	**12h**	**24h**	**36h**	**48h**

run1	Undetermined	Undetermined	29,85	29,90	38,31	35,92	35,68	27,26	30,41	37,53	38,51	38,84	26,54	33,65	29,43
run1	Undetermined	Undetermined	29,19	29,77	39,25	36,10	35,88	26,94	30,06	37,44	38,40	39,91	26,35	33,81	29,60
run1	Undetermined	Undetermined	29,93	29,47	Undetermined	35,75	35,52	26,84	30,25	38,01	38,62	38,91	26,50	33,40	30,17
run2	38,70	Undetermined	29,73	29,81	39,70	35,11	38,28	23,47	29,36	36,17	32,81	34,26	25,11	23,87	26,24
run2	39,38	Undetermined	29,49	29,35	40,54	35,49	38,74	25,18	29,10	36,14	32,67	34,91	24,94	24,57	25,93
run2	41,93	Undetermined	29,83	29,35	40,17	34,92	37,45	Undetermined	29,05	35,93	32,20	34,14	25,10	24,69	25,82
run3	41,72	Undetermined	28,93	29,68	37,91	33,52	33,54	30,21	26,01	33,00	36,93	34,84	25,40	26,27	32,91
run3	40,84	Undetermined	29,09	29,57	38,31	33,47	32,33	30,07	26,24	32,91	35,92	34,69	25,89	25,94	32,49
run3	41,85	Undetermined	29,01	29,28	37,09	33,54	32,51	29,90	26,01	32,70	35,79	34,37	25,84	26,39	32,55

***Tal* standard deviation**														
L2					**E**					**US151**				
2h	**12h**	**24h**	**36h**	**48h**	**2h**	**12h**	**24h**	**36h**	**48h**	**2h**	**12h**	**24h**	**36h**	**48h**

run1	1,48		0,07	0,14	0,79	0,18	0,18	0,22	0,18	0,30	0,11	0,60	0,10	0,21	0,39
run2	1,70		0,18	0,27	0,42	0,29	0,65	1,22	0,17	0,13		0,42	0,28	0,45	0,22
run3	0,19		0,08	0,28	0,62	0,04	0,65	0,16	0,13	0,16		0,24	0,27	0,23	

	***hctA* CT values**														
	L2					**E**					**US151**				
	2h	**12h**	**24h**	**36h**	**48h**	**2h**	**12h**	**24h**	**36h**	**48h**	**2h**	**12h**	**24h**	**36h**	**48h**
run1	42,12	42,60	25,92	25,33	40,61	37,31	37,36	22,90	31,39	35,10	40,32	41,27	26,22	26,12	36,71
run1	43,95	43,67	26,02	25,62	40,48	37,82	36,93	23,80	31,65	35,52	39,73	40,89	26,35	26,06	36,98
run1	42,73	41,64	25,33	25,14	39,49	37,70	36,67	23,58	31,22	35,40	40,00	40,86	26,68	25,73	37,01
run2	42,42	41,56	24,87	24,59	35,97	38,97	41,12	25,53	29,96	38,69	44,12	43,61	28,85	28,93	39,24
run2	42,70	41,93	24,63	24,59	36,71	38,04	39,45	25,91	29,93	38,52	Undetermined	43,51	28,81	29,03	39,31
run2	43,96	41,02	25,03	24,46	36,59	40,17	40,02	26,16	29,94	38,54	43,80	42,66	29,27	28,72	40,32
run3	44,92	41,94	25,93	27,93	39,24	39,77	40,42	28,30	29,45	37,93	46,93	43,90	27,96	28,22	38,13
run3	Undertimed	42,79	26,37	27,85	39,24	39,76	41,02	27,76	29,47	38,28	45,35	43,93	28,16	28,26	38,26
run3	43,97	42,54	26,45	27,77	39,51	39,68	40,92	29,41	29,19	38,28	45,36	Undetermined	28,16	27,98	37,97

	***hctA* standard deviation**														
	L2					**E**					**US151**				
	2h	**12h**	**24h**	**36h**	**48h**	**2h**	**12h**	**24h**	**36h**	**48h**	**2h**	**12h**	**24h**	**36h**	**48h**
run1	0,89	0,89	0,89	0,89	0,89	0,27	0,35	0,47	0,24	0,22	0,29	0,23	0,24	0,21	0,17
run2	0,82	0,46	0,20	0,07	0,40	1,07	0,85	0,32	0,13	0,09	0,23	0,52	0,25	0,16	0,60
run3	0,67	0,44	0,28	0,08	0,16	0,05	0,32	0,84	0,15	0,20	0,91	0,03	0,12	0,15	0,15

	***OmcB* CT values**														
	L2					**E**					**US151**				
	2h	**12h**	**24h**	**36h**	**48h**	**2h**	**12h**	**24h**	**36h**	**48h**	**2h**	**12h**	**24h**	**36h**	**48h**
run1	34,94	Undetermined	30,09	30,53	40,01	37,27	36,27	27,34	30,77	38,76	39,33	40,14	26,82	35,82	29,37
run1	37,82	Undetermined	30,15	30,53	40,42	36,93	36,80	27,40	30,86	38,30	40,28	38,82	27,14	35,63	37,44
run1	36,97	Undetermined	30,23	30,30	41,27	36,61	36,42	27,69	30,70	38,46	41,82	39,56	26,93	35,38	43,30
run2	39,15	Undetermined	29,94	29,94	30,03	37,15	38,92	24,79	29,62	37,39	34,23	35,93	25,66	25,50	27,03
run2	39,54	Undetermined	29,86	29,96	30,86	37,12	38,92	24,95	29,26	36,45	34,13	35,76	25,72	25,75	27,18

run2	39,45	Undetermined	29,84	29,79	Undetermined	38,82	38,41	25,09	29,41	39,45	34,25	35,93	25,82	25,86	26,92
run3	35,57	42,05	29,79	24,77	40,02	33,96	34,50	31,69	27,35	34,70	Undetermined	35,11	26,14	26,62	26,87
run3	35,06	42,07	29,73	24,32	39,96	34,14	33,94	30,98	26,82	34,54	37,98	35,26	26,33	26,55	27,02
run3	35,38	41,94	28,93	24,58	39,04	35,57	33,75	31,83	27,58	33,66	37,77	35,95	25,72	29,77	26,94

	***OmcB* standard deviation**														
	L2					**E**					**US151**				
	2h	**12h**	**24h**	**36h**	**48h**	**2h**	**12h**	**24h**	**36h**	**48h**	**2h**	**12h**	**24h**	**36h**	**48h**
run1	1,48		0,07	0,14	0,79	0,33	0,27	0,19	0,08	0,23	1,26	0,66	0,16	0,22	6,99
run2	0,21		0,05	0,09	0,59	0,97	0,30	0,15	0,18	1,54	0,06	0,10	0,08	0,18	0,13
run3		0,09	0,48	0,23	0,49	0,88	0,39	0,46	0,39	0,56	0,15	0,45	0,31	0,04	0,23

2. HaCaT 33°C C_T and standard deviation values

	***16SrRNA* CT values**																			
	L2							**E**							**US151**						
	2h	**12h**	**24h**	**36h**	**48h**	**60h**	**72h**	**2h**	**12h**	**24h**	**36h**	**48h**	**60h**	**72h**	**2h**	**12h**	**24h**	**36h**	**48h**	**60h**	**72h**
run 1	32, 55	32, 60	40, 55	39, 95	43, 28	37, 88	32, 69	40, 27	41, 67	39, 71	41, 92	42, 48	42, 00	40, 42	36, 89	38, 78	40, 57	40, 34	42, 78	39, 89	37, 89
run 1	32, 43	32, 30	41, 94	39, 76	42, 07	37, 39	32, 87	41, 10	42, 46	40, 59	41, 51	41, 59	42, 07	40, 57	36, 34	38, 56	41, 03	40, 46	43, 89	39, 89	38, 46
run 1	32, 31	31, 80	41, 06	39, 98	43, 97	37, 22	33, 00	41, 79	41, 17	40, 48	42, 97	43, 35	41, 58	40, 46	35, 68	38, 35	40, 22	40, 35	42, 89	39, 12	38, 34
run 2	33, 55	33, 46	39, 09	39, 46	41, 38	35, 68	33, 89	40, 22	40, 37	39, 33	40, 23	42, 78	41, 56	40, 23	35, 45	35, 68	41, 77	41, 23	42, 90	40, 69	39, 66
run 2	32, 79	33, 46	39, 78	38, 46	41, 27	35, 24	33, 90	40, 48	40, 46	39, 27	40, 46	42, 46	41, 25	41, 46	34, 91	36, 35	41, 78	40, 56	41, 67	39, 57	39, 10
run 2	33, 21	32, 56	39, 21	38, 88	41, 26	35, 56	33, 89	40, 34	41, 01	38, 26	41, 09	41, 55	41, 89	41, 23	35, 46	35, 76	40, 46	41, 98	42, 01	40, 57	38, 99
run 3	33, 80	30, 03	29, 81	28, 01	29, 00	42, 12	20, 11	31, 54	31, 03	35, 02	28, 10	33, 61	32, 60	32, 03	33, 73	34, 28	32, 57	34, 29	35, 63	30, 36	31, 01
run 3	32, 34	29, 81	29, 64	28, 04	28, 83	41, 00	19, 90	31, 39	31, 23	34, 88	28, 68	33, 39	32, 53	31, 97	33, 27	34, 45	32, 16	34, 25	35, 26	30, 26	31, 17
run 3	34, 04	29, 79	30, 14	28, 56	28, 91	41, 89	22, 69	31, 11	31, 33	35, 27	28, 14	33, 67	32, 60	31, 95	33, 14	34, 35	32, 20	34, 29	35, 28	30, 46	31, 35

	***16SrRNA* standard deviation**																		
	L2							**E**							**US151**						
	2h	**12h**	**24h**	**36h**	**48h**	**60h**	**72h**	**2h**	**12h**	**24h**	**36h**	**48h**	**60h**	**72h**	**2h**	**12h**	**24h**	**36h**	**48h**	**60h**	**72h**
run 1	0,34	0,09	0,45	0,47	0,34	0,81	0,75	0,07	0,23	0,17	0,45	0,11	0,06	0,07	0,65	0,56	0,02	0,01	0,33	0,02	0,06
run 2	0,56	0,12	0,26	0,33	0,08	0,53	0,94	0,08	0,43	0,23	0,77	0,23	0,05	0,09	0,45	0,22	0,05	0,04	0,56	0,09	0,04
run 3	0,92	0,13	0,25	0,31	0,09	0,79	1,55	0,22	0,15	0,20	0,32	0,15	0,04	0,04	0,21	0,13	0,53	0,34	0,98	0,07	0,02

	***groEL -1* CT values**																		
	L2							**E**							**US151**						
	2h	**12h**	**24h**	**36h**	**48h**	**60h**	**72h**	**2h**	**12h**	**24h**	**36h**	**48h**	**60h**	**72h**	**2h**	**12h**	**24h**	**36h**	**48h**	**60h**	**72h**
run 1	37,95	36,88	41,99	40,92	41,58	39,31	39,85	39,57	41,90	39,25	39,74	40,12	39,29	38,22	40,45	41,89	41,36	39,46	37,88	35,24	34,97
run 1	37,61	36,95	42,36	39,85	41,29	41,99	38,94	38,90	39,50	38,56	40,69	40,89	39,35	40,24	40,81	41,24	40,78	38,24	37,10	35,09	35,06
run 1	37,98	36,68	40,24	40,56	41,82	40,92	39,51	39,28	40,54	39,55	40,66	41,93	40,42	39,58	41,57	41,41	39,92	39,46	38,18	35,77	35,26
run 2	35,67	37,22	41,25	41,01	40,57	39,45	40,35	40,35	40,57	40,68	40,57	40,35	40,86	40,46	38,35	40,46	39,67	39,46	39,55	34,78	35,56
run 2	35,99	36,78	41,67	40,99	41,35	39,01	40,46	40,36	40,32	40,33	40,35	40,23	39,65	40,22	38,30	40,56	39,46	38,34	39,35	34,68	35,78

run 2	35,29	37,01	41,45	40,56	41,88	39,67	39,23	40,57	40,66	39,20	40,46	41,35	39,44	40,36	38,46	40,33	40,46	38,56	39,46	35,18	35,68
run 3	35,76	31,93	32,06	30,41	30,43	41,35	32,08	29,53	31,84	29,68	29,60	30,83	34,49	33,30	31,36	35,35	29,75	33,63	34,18	34,89	33,78
run 3	35,62	31,69	31,97	30,27	30,41	41,33	32,15	29,38	31,52	29,77	29,64	30,94	34,67	33,59	31,67	35,13	29,57	33,98	34,56	34,02	33,89
run 3	35,36	31,55	32,20	30,37	30,39	41,23	32,21	29,46	31,64	29,80	29,56	30,86	34,50	33,58	31,22	35,74	29,47	33,75	34,19	34,85	33,68

	***groEL-1* standard deviation**																			
	L2							**E**							**US151**					
	2h	**12h**	**24h**	**36h**	**48h**	**60h**	**72h**	**2h**	**12h**	**24h**	**36h**	**48h**	**60h**	**72h**	**2h**	**12h**	**24h**	**36h**	**48h**	**60h**	**72h**
run 1	0,23	0,22	0,08	0,56	0,20	0,39	0,28	0,25	0,20	0,21	0,54	0,21	0,33	0,03	0,37	0,25	0,26	0,25	0,22	0,27	0,30
run 2	0,27	0,38	0,17	0,33	0,22	0,28	0,33	0,38	0,10	0,25	0,35	0,23	0,32	0,25	0,26	0,35	0,29	0,24	0,12	0,25	0,29
run 3	0,20	0,19	0,12	0,07	0,02	0,02	0,07	0,08	0,16	0,06	0,04	0,06	0,10	0,16	0,25	0,03	0,01	0,23	0,12	0,27	0,11

	***IncB* CT values**																			
	L2							**E**							**US151**						
	2h	**12h**	**24h**	**36h**	**48h**	**60h**	**72h**	**2h**	**12h**	**24h**	**36h**	**48h**	**60h**	**72h**	**2h**	**12h**	**24h**	**36h**	**48h**	**60h**	**72h**
run 1	39,39	40,67	43,95	42,85	41,26	43,45	39,75		34,73	36,07	39,53	39,73	40,50	39,01	34,35		40,56	42,45	39,54	40,33	
run 1	38,98	41,15	44,49	42,84	43,75	43,62	39,20		34,53	35,76	39,47	40,31	40,43	39,43	34,13	37,34	40,36	42,35	40,65	40,12	37,23
run 1	40,58	40,93		43,31	42,34		38,18		34,53	34,76	38,63	39,29	39,78	38,86	34,46	37,56	40,60	41,97	40,15	40,35	37,13
run 2	40,23		42,56	43,23	41,23	44,23			33,45	37,35	39,67	40,56	40,13	38,35		38,23	41,35	40,45	39,46	39,57	38,56
run 2	40,34	40,23	42,12	43,56	41,35	43,67	38,35		34,98	37,56	39,14	40,13	40,46	38,23	35,46	38,45	41,45	40,44	39,91	39,56	38,65
run 2	40,23	39,23	43,25	43,89	41,45	43,87	39,42		34,98	37,30	39,25	40,23	40,43	38,12	35,79	37,98	40,56		40,23	40,10	39,46
run 3	37,67	33,32	34,21	31,16	31,92		23,92		33,34	31,11	30,73	31,93	25,70	24,57	33,46	29,23	31,34	34,97	30,26	29,45	34,55
run 3	37,13	33,93	34,50	32,10	32,25	39,42	24,14		33,21	30,95	30,86	31,96	25,79	24,64	33,09	29,09	31,36	34,29	30,24	29,46	34,25
run 3	37,85	34,10	34,10	32,01	32,25	40,87	23,93		33,39	30,97	30,60	31,99	25,80	24,52	33,11	30,01	31,34	34,68	31,00	29,44	34,89

	***incB* standard deviation**																		
	L2							**E**							**US151**						
	2h	**12h**	**24h**	**36h**	**48h**	**60h**	**72h**	**2h**	**12h**	**24h**	**36h**	**48h**	**60h**	**72h**	**2h**	**12h**	**24h**	**36h**	**48h**	**60h**	**72h**
run 1	0,28	0,33	0,43	0,25	0,36	1,11	0,81		0,26	0,20	0,37	1,13	0,02	0,56	0,13	0,46	0,38	0,28	0,11	0,89	0,45
run 2	0,03	0,38	0,06	0,02	0,36	1,03	0,03		0,39	0,04	0,01	0,09	0,31	0,03	0,04	0,09	0,26	0,07	0,10	0,07	0,04
run 3	0,38	0,41	0,21	0,52	0,19	1,02	0,13		0,09	0,09	0,13	0,03	0,06	0,06	0,25	0,45	0,29	0,18	0,05	0,03	0,02

	***Pyk-F* CT values**																				
	L2							**E**							**US151**						
	2h	**12h**	**24h**	**36h**	**48h**	**60h**	**72h**	**2h**	**12h**	**24h**	**36h**	**48h**	**60h**	**72h**	**2h**	**12h**	**24h**	**36h**	**48h**	**60h**	**72h**
run 1	37,79	36,81	39,25	40,43	39,80	40,65	39,16		40,20	40,78	39,50	41,69	39,05	39,94			38,45	40,35	39,53	36,19	35,67
run 1	37,96	36,68	39,25	40,71	40,59	39,93	38,21		40,13	40,82	41,81	40,11	40,13	39,63			37,22	40,44	40,23	36,46	35,52
run 1	37,59	36,73	40,74	41,93	40,10	40,42	38,84		40,69	40,84	41,81	40,50	39,91	40,65			37,23	40,24	40,12	35,46	36,45

run 2	38,12	35,87		40,34	39,24	40,43	39,87		42,67	40,34	39,56		39,56	38,34			36,56	41,35	41,01	36,56	37,55
run 2	38,26	36,45	40,36	40,23	39,46	39,98			41,34	40,25	39,34	40,20	39,24	39,23			37,45	41,23	40,24	35,55	37,23
run 2	37,56	35,20	40,23	40,12	40,35	40,24	39,43		41,89	40,33	39,02	40,26	39,03				37,23	40,98	39,35	35,89	37,23
run 3	35,68	31,48	32,08	30,36	30,39	39,31	38,32		31,75	29,24	29,37	30,45	24,35	23,16			34,82	32,26	33,75	34,28	33,26
run 3	35,94	31,96	32,11	30,57	30,51	40,32	38,45		31,68	29,55	29,60	30,56	24,30	23,22			34,56	32,56	33,73	34,36	33,46
run 3	35,71	33,90	32,34	30,23	30,31	39,46			31,40	29,62	29,38	30,44	24,25	23,19			34,35	32,57	33,27	34,78	33,24

	***Pyk-F* standard deviation**																			
	L2							**E**							**US151**						
	2h	**12h**	**24h**	**36h**	**48h**	**60h**	**72h**	**2h**	**12h**	**24h**	**36h**	**48h**	**60h**	**72h**	**2h**	**12h**	**24h**	**36h**	**48h**	**60h**	**72h**
run1	0,21	0,40	0,24	0,21	0,04	0,21	0,23		0,34	0,03	0,34	0,02	0,05	0,52			0,06	0,56	0,38	0,46	0,02
run2	0,35	0,27	0,27	0,38	0,56	0,36	0,25		0,19	0,06	0,56	0,03	0,35	0,25			0,21	0,27	0,05	0,35	0,05
run3	0,14	0,28	0,14	0,17	0,06	0,00	0,22		0,18	0,20	0,13	0,07	0,05	0,03			0,13	0,02	0,05	0,15	0,03

	***Tal* CT values**																			
	L2							**E**							**US151**						
	2h	**12h**	**24h**	**36h**	**48h**	**60h**	**72h**	**2h**	**12h**	**24h**	**36h**	**48h**	**60h**	**72h**	**2h**	**12h**	**24h**	**36h**	**48h**	**60h**	**72h**
run 1	38,49	38,05	41,30	40,65	39,58	41,01	38,94				39,65	39,95	41,39	40,74	40,24		41,27	40,68		40,67	37,86
run 1	38,25	37,96	40,37		39,96	40,28	40,34				39,48	38,70	41,21	41,25	39,75	39,45		40,97	39,58	41,89	37,87
run 1	38,01	38,82	41,04	40,38	42,45		40,00				39,00	39,37	40,80	39,92	39,75	39,74	40,56	41,08	39,97	40,93	37,55
run 2	36,56	39,35	40,45	40,27	39,35	40,90	40,68				38,22	39,75	41,35	42,35	39,57	38,45	40,94	40,72	40,76	41,49	35,84
run 2	36,98	39,28	41,56	41,90	38,91	40,23	40,13				38,91	39,10	41,10	40,44	39,65	39,91	39,85	39,58	40,20	40,34	35,72
run 2	37,89	40,07	41,65	41,67	39,35	40,40	40,78				38,36	39,23	41,56	40,13		38,35	39,84	39,47	39,56	40,13	35,81
run 3	34,23	33,36	34,25	29,46	31,65	35,00	32,46				34,83	32,88	35,01	33,74	31,76	29,92	30,07	30,47	28,30	23,87	23,67
run 3	35,09	33,34	34,68	29,34	31,89	35,11	32,16				34,89	32,46	34,84	33,36	31,59	29,62	30,85	30,47	28,27	23,90	23,57

run 3	35,01	33,47	34,78	29,55	31,34	35,09	32,78				34,56	32,99	34,63	33,49	31,59	29,54	30,16	30,46	28,39	23,91	23,50

	***Tal* standard deviation**																			
	L2							**E**							**US151**						
	2h	**12h**	**24h**	**36h**	**48h**	**60h**	**72h**	**2h**	**12h**	**24h**	**36h**	**48h**	**60h**	**72h**	**2h**	**12h**	**24h**	**36h**	**48h**	**60h**	**72h**
run1	0,34	0,52	0,52	0,73	0,65	1,22	0,74				0,02	0,30	0,67	0,06	0,67	0,38	0,35	0,08	0,07	0,21	0,45
run2	0,01	0,18	0,28	0,05	0,01	0,09	0,04				0,35	0,04	0,09	0,31	0,09	0,04	0,21	0,16	0,39	0,09	0,08
run3	0,04	0,15	0,25	0,04	0,03	0,07	0,02				0,07	0,03	0,12	0,45	0,49	0,20	0,43	0,10	0,06	0,02	0,08

	***hctA* CT values**																			
	L2							**E**							**US151**						
	2h	**12h**	**24h**	**36h**	**48h**	**60h**	**72h**	**2h**	**12h**	**24h**	**36h**	**48h**	**60h**	**72h**	**2h**	**12h**	**24h**	**36h**	**48h**	**60h**	**72h**
run 1	42,17	40,33	42,44	45,94	42,95	43,93	43,34		45,05	42,94	44,60	44,54		37,68	40,25		42,55	41,90	42,18	38,15	38,56
run 1	42,22	39,59		44,00	43,95	44,26	41,20		45,22	44,31	44,57	46,79	42,90	38,01	40,25		42,91	41,24	41,69	39,21	38,24
run 1	41,43	40,02	43,90	42,48	44,02	41,97	42,43		44,57	45,32	43,98	45,85	42,40	37,88	41,67		41,33	41,24	42,45	39,46	38,56

run 2	41,23	40,23	41,23		43,09	43,23	40,35		45,54	45,35	43,63	45,67	41,23	38,23			42,72	43,97	43,19	39,09	38,77
run 2	41,02	40,23	42,87	40,23	43,98	41,34	40,23		43,54	45,23	44,34	45,33	42,67	38,23	42,78		41,09	41,36		38,68	39,25
run 2	41,45	40,43	42,78	40,44	42,34	40,34	40,33		43,66	44,78	44,34		42,76	38,01	42,88		41,45	43,01	43,95	39,27	39,59
run 3	34,23	29,35	33,09	28,45	30,56	30,23	33,65		34,65	35,00	35,09	35,67	33,75	31,94	34,48		32,22	32,87	30,77	34,98	34,96
run 3	34,55	29,25	32,96	28,56	30,24	31,45	33,84		35,00	34,98	35,65	35,09	33,98	31,25	33,18		32,20	32,92	30,87	35,02	35,00
run 3	34,67	29,46	33,45	28,98	30,45	30,87	33,56		34,64	34,91	35,16	36,00	33,76	31,55	34,56		32,71	32,89	30,75	34,95	35,12

	***hctA* standard deviation**																			
	L2							**E**							**US151**					
	2h	**12h**	**24h**	**36h**	**48h**	**60h**	**72h**	**2h**	**12h**	**24h**	**36h**	**48h**	**60h**	**72h**	**2h**	**12h**	**24h**	**36h**	**48h**	**60h**	**72h**
run 1	0,46	0,54	0,05	0,23	0,13	0,29	0,08		0,11	0,29	0,20	0,31	0,08	0,40	0,04		0,38	0,46	0,08	0,09	0,65
run 2	0,38	0,07	0,35	0,12	0,56	0,27	0,37		0,02	0,35	0,26	0,34	0,03	0,06	0,23		0,06	0,38	0,20	0,17	0,04
run 3	0,23	0,02	0,03	0,15	0,34	0,22	0,19		0,04	0,25	0,39	0,25	0,06	0,04	0,12		0,29	0,03	0,06	0,04	0,08

	***OmcB* CT values**																			
	L2							**E**							**US151**					
	2h	**12h**	**24h**	**36h**	**48h**	**60h**	**72h**	**2 h**	**12 h**	**24h**	**36h**	**48h**	**60h**	**72h**	**2h**	**12h**	**24h**	**36h**	**48h**	**60h**	**72h**
run 1	39,94	39,22	41,13	43,15	39,93	40,77	39,30			42,02	41,98	43,95	40,27	42,76	38,23		40,56	43,56	40,46	39,46	38,96
run 1	39,52	39,25	40,30	40,45	38,99	41,32	42,42			40,82	41,98	42,17	41,64	42,76	38,46	39,35	40,78	43,98	40,86	39,08	38,94
run 1	40,56	40,70		42,37	39,57	40,46	39,40			41,93	42,17	39,95	40,01	42,03	39,78	39,10	40,13	44,77	40,76	39,83	38,87
run 2	39,23	40,55	40,74	42,66	39,99	40,35	42,45			40,40	41,23	43,66	41,89	40,76	39,00	40,44	43,55	43,90	40,28	38,58	39,66
run 2	39,79	40,29	41,98	41,91	40,35	40,09	42,35			40,56	41,01	43,90	41,57	41,44	39,26	39,95	42,99		40,34	38,89	39,78
run 2	38,99	40,71	41,37	41,56	38,36	41,65	41,87			40,27	40,23	43,65	41,06	40,77	39,67	39,65	42,10	42,89	40,68	39,76	39,89
run 3	31,35	34,45	30,55	33,69	28,46	32,16	34,45			33,33	35,89	34,28	31,64	33,56	32,94	30,59	30,86	31,16	38,97	34,66	34,29
run 3	31,66	34,78	30,24	33,78	28,46	32,98	34,89			33,78	35,56	34,35	31,14	33,94	32,77	30,47	30,83	31,22	38,98	34,49	24,09
run 3	31,84	34,79	30,25	33,12	28,36	32,57	34,44			33,90	35,28	34,79	31,46	33,67	32,61	30,44	30,92	31,20	38,99	34,61	34,30

***omcB* standard deviation**

	L2							E							US151						
	2h	**12h**	**24h**	**36h**	**48h**	**60h**	**72h**	**2h**	**12h**	**24h**	**36h**	**48h**	**60h**	**72h**	**2h**	**12h**	**24h**	**36h**	**48h**	**60h**	**72h**
run 1	0,57	0,28	0,21	0,55	0,63	0,13	0,28			0,67	0,11	0,01	0,27	0,38	0,24	0,06	0,26	0,39	0,48	0,67	0,11
run 2	0,07	0,03	0,12	0,03	0,09	0,03	0,01			0,16	0,23	0,06	0,10	0,31	0,45	0,13	0,35	0,19	0,27	0,09	0,26
run 3	0,03	0,12	0,26	0,27	0,07	0,01	0,03			0,30	0,26	0,04	0,18	0,27	0,16	0,08	0,04	0,03	0,01	0,09	0,12

3. HeLa 37°C C_T and standard deviation values

	***16SrRNA* CT values**														
	L2					**E**					**US151**				
	2h	**12h**	**24h**	**36h**	**48h**	**2h**	**12h**	**24h**	**36h**	**48h**	**2h**	**12h**	**24h**	**36h**	**48h**
run1	32,12	30,95	30,83	30,89	34,00	36,25	35,09	27,53	37,96	32,49	32,85	32,23	31,64	35,81	32,76
run1	31,97	31,01	30,26	31,13	33,22	36,84	35,81	27,24	38,30	32,96	31,98	29,88	31,74	35,80	33,28
run1	30,96	30,30	30,27	31,18	34,10	37,56	34,71	28,15	37,87	32,23	32,97	31,49	31,77	35,69	32,72
run2	33,51	33,41	33,29	33,77	33,88	36,23	35,35	27,21	37,77	32,43	32,77	31,43	31,33	35,23	33,22
run2	34,10	33,07	33,20	34,24	33,92	36,23	35,21	27,98	37,34	32,44	32,65	31,65	31,41	35,09	32,98
run2	33,31	32,94	33,29	33,71	33,80	36,87	35,87	27,34	37,65	32,76	32,55	31,44	31,21	35,44	33,11
run3	32,16	32,19	32,40	31,98	32,51	37,01	34,21	28,11	38,11	33,11	33,54	32,33	31,32	35,97	32,87
run3	32,11	32,41	32,77	31,99	32,42	37,11	34,54	28,32	38,23	32,54	33,13	32,16	31,65	35,56	33,15

run3	32,02	32,48	31,68	31,91	32,68	37,09	34,87	28,19	38,74	32,66	33,23	33,97	31,43	35,33	33,71

	***16SrRNA* standard deviation**														
	L2					**E**					**US151**				
	2h	**12h**	**24h**	**36h**	**48h**	**2h**	**12h**	**24h**	**36h**	**48h**	**2h**	**12h**	**24h**	**36h**	**48h**
run1	0,63	0,39	0,33	0,15	0,67	0,65	0,56	0,47	0,49	0,79	0,54	1,20	0,06	0,07	0,31
run2	0,07	0,15	0,55	0,04	0,13	0,03	0,02	0,03	0,32	0,34	0,07	0,23	0,04	0,05	0,05
run3	0,03	0,01	0,43	0,04	0,05	0,12	0,32	0,12	0,34	0,33	0,05	0,04	0,05	0,06	0,34

	***groel-1* CT values**														
	L2					**E**					**US151**				
	2h	**12h**	**24h**	**36h**	**48h**	**2h**	**12h**	**24h**	**36h**	**48h**	**2h**	**12h**	**24h**	**36h**	**48h**
run1	39,23	40,89	40,12	31,74	37,911	33,25	35,26	37,11	31,22	34,24	35,47	35,27	38,03	37,12	40,99
run1	39,52	39,26	40,67	31,90	36,93	33,76	35,56	37,23	32,01	34,64	35,61	35,06	37,55	36,99	40,12
run1	39,36	39,42	41,80	31,65	37,98	33,22	35,22	37,33	31,34	34,66	35,06	34,96	37,10	36,95	39,92
run2	39,25	40,11	40,23	31,65	37,33	34,13	35,45	37,92	31,98	34,12	35,02	34,99	37,98	36,11	40,55
run2	39,22	40,46	40,55	31,33	37,82	34,11	35,77	37,12	31,34	34,76	35,76	34,78	37,66	36,85	40,34
run2	39,67	40,23	40,15	31,68	37,23	34,02	34,99	37,54	32,81	34,36	35,22	34,22	37,23	36,33	40,66
run3	39,44	39,23	40,45	31,83	37,91	33,23	35,22	37,55	31,45	34,12	35,01	35,76	37,33	36,36	40,23
run3	39,23	39,12	40,12	31,22	37,44	33,76	35,01	35,62	31,55	34,65	35,9	35,11	37,48	36,12	40,88
run3	39,88	39,32	40,11	31,09	37,76	33,21	35,22	35,12	31,22	34,22	35,56	35,77	37,58	36,92	40,24

	***groEL-1* standard deviation**														
	L2					**E**					**US151**				
	2h	**12h**	**24h**	**36h**	**48h**	**2h**	**12h**	**24h**	**36h**	**48h**	**2h**	**12h**	**24h**	**36h**	**48h**
run1	0,15	0,90	0,80	0,13	0,04	0,08	0,04	0,07	0,09	0,12	0,29	0,16	0,47	0,09	0,76
run2	0,04	0,01	0,04	0,03	0,23	0,06	0,03	0,07	0,04	0,01	0,04	0,02	0,05	0,06	0,05
run3	0,03	0,15	0,05	0,07	0,09	0,03	0,01	0,04	0,08	0,05	0,03	0,01	0,03	0,03	0,05

	***Pyk-F* CT values**														
	L2					**E**					**US151**				
	2h	**12h**	**24h**	**36h**	**48h**	**2h**	**12h**	**24h**	**36h**	**48h**	**2h**	**12h**	**24h**	**36h**	**48h**
run1		41,68	41,74	31,61	36,58		36,95	34,51	45,51	37,08		38,24	40,49	36,71	40,21
run1		41,79	41,32	31,81	35,74		36,91	34,69	45,00	36,41		37,94	40,21	36,74	40,23
run1		41,90	40,42	30,92	36,53		36,22	34,87	45,97	37,98		39,42	39,32	36,49	41,18
run2		41,53	40,56	31,56	35,65		35,98	34,27	44,23	36,25		38,34	40,21	37,23	39,34
run2		40,98	39,99	30,98	35,33		35,23	35,01	45,22	36,19		38,34	40,22	37,12	39,33
run2		40,69	41,01	30,65	36,56		35,87	35,56	45,23	36,34		38,64	40,74	37,32	39,65
run3		41,45	39,98	31,34	36,22		35,21	34,31	44,09	36,98		39,12	39,85	36,54	40,12
run3		41,09	39,84	31,67	35,23		36,33	34,26	44,65	36,32		39,54	40,13	36,87	40,11

run3		40,97	39,45	31,02	35,61		36,34	34,61	44,32	36,18		38,97	39,34	36,33	40,21

	Pyk-F standard deviation														
	L2					**E**					**US151**				
	2h	**12h**	**24h**	**36h**	**48h**	**2h**	**12h**	**24h**	**36h**	**48h**	**2h**	**12h**	**24h**	**36h**	**48h**
run1		0,13	0,93	0,47	0,11		0,41	0,18	0,23	0,37		0,78	0,83	0,14	0,69
run2		0,04	0,05	0,07	0,18		0,15	0,03	0,07	0,08		0,13	0,07	0,05	0,06
run3		0,02	0,07	0,06	0,09		0,13	0,04	0,06	3,00		0,14	0,03	0,02	0,02

	***hctA* CT values**														
	L2					**E**					**US151**				
	2h	**12h**	**24h**	**36h**	**48h**	**2h**	**12h**	**24h**	**36h**	**48h**	**2h**	**12h**	**24h**	**36h**	**48h**
run1			44,00	34,25	32,86			35,16	45,04	37,54			43,16	36,09	43,00
run1			44,01	34,23	32,96			34,92	44,91	38,35			42,91	36,13	43,86
run1			44,11	33,92	32,66			35,50	45,36	37,15			43,07	35,99	43,91
run2			44,90	35,40	36,73			35,02	45,56	36,96			43,74	35,46	42,35
run2			44,76	35,53	36,87			35,26	45,62	37,50			44,01	35,10	43,09
run2			44,49	35,52	37,69			35,56	45,09	37,27			44,46	35,55	43,24
run3			43,20	33,37	31,86			34,75	44,46	37,09			43,89	36,71	42,12

run3			44,29	33,16	30,97			34,55	44,71	36,44			43,65	36,09	42,88
run3			45,44	32,97	31,35			35,01	45,34	37,02			44,46	35,68	43,00

	***hctA* standard deviation**														
	L2					**E**					**US151**				
	2h	**12h**	**24h**	**36h**	**48h**	**2h**	**12h**	**24h**	**36h**	**48h**	**2h**	**12h**	**24h**	**36h**	**48h**
run1			0,08	0,04	0,07			0,29	0,23	0,61			1,12	0,20	0,45
run2			0,11	0,07	0,29			0,07	0,09	0,05			0,12	0,05	
run3			0,09	0,09	0,08			0,04	0,12	0,08			0,14	0,07	0,04